Science Advances

AAAS

advances.sciencemag.org/cgi/content/full/3/5/e1601693/DC1

Supplementary Materials for

Miocene flooding events of western Amazonia

Carlos Jaramillo, Ingrid Romero, Carlos D'Apolito, German Bayona, Edward Duarte, Stephen Louwye, Jaime Escobar, Javier Luque, Jorge D. Carrillo-Briceño, Vladimir Zapata, Alejandro Mora, Stefan Schouten, Michael Zavada, Guy Harrington, John Ortiz, Frank P. Wesselingh

Published 3 May 2017, *Sci. Adv.* **3**, e1601693 (2017)
DOI: 10.1126/sciadv.1601693

The PDF file includes:

- fig. S9. Stratigraphic correlation of the two major marine incursions (EMI and MMI) from the Saltarin well to the northernmost expression of the Vaupés Arch in the subsurface (well I).
- fig. S10. Stratigraphic correlation of the two major marine incursions (EMI and MMI) along the northern Amazonas/Solimões Basin.
- fig. S11. Graphic correlation between the standard composite section of Jaramillo *et al.* (*56*) and core Saltarin.
- fig. S12. Graphic correlation between the standard composite section of Jaramillo *et al.* (*56*) and core 105-AM.
- fig. S13. Seismic profiles in the Llanos Basin (see location in fig. S2; interpretation only at one extreme of the line) illustrate the seismic facies of the two marine incursions (EMI and MMI).
- fig. S14. Interpreted 2D seismic profiles showing the contrasting difference of seismic facies between undifferentiated Cenozoic and Cretaceous units in the Amazonas/Solimões Basin (see fig. S2 for the location of seismic lines).
- fig. S15. Graphic correlation between the cores Saltarin and 105-AM.
- fig. S16. Carbon isotope data ($\delta^{13}C$) versus stratigraphic position in core Saltarin on the left panel.
- fig. S17. Carbon isotope data ($\delta^{13}C$) versus stratigraphic position in core 105-AM.
- fig. S18. Photographs of shells from core 105-AM.
- fig. S19. Molluscan biostratigraphy of core 105-AM.
- Legends for tables S1 to S12
- file S1. GPlates project.
- file S2. R code.
- file S3. Graphic correlation.
- file S4. Biostratigraphic and sequence stratigraphic events.
- file S5. Lithological description of the cores 105-AM and Saltarin.
- file S6. Excel tables.
- References (*65–134*, *138–185*)

Other Supplementary Material for this manuscript includes the following:
(available at advances.sciencemag.org/cgi/content/full/3/5/e1601693/DC1)

- table S1 (Microsoft Excel format). Palynomorph counts for samples analyzed in core Saltarin.
- table S2 (Microsoft Excel format). Palynomorph counts for samples analyzed in core 105-AM.
- table S3 (Microsoft Excel format). Summary of palynological count data.
- table S4 (Microsoft Excel format). BIT index for Saltarin samples.
- table S5 (Microsoft Excel format). Geographic coordinates and information of outcrops and wells (coordinate system WGS 1984) used in this study.
- table S6 (Microsoft Excel format). Geographic coordinates and information of 2D seismic lines (coordinate system WGS 1984) used in this study.
- table S7 (Microsoft Excel format). Summary of lithological and palynological indicators for depositional environment interpretation of the Saltarin well.

- table S8 (Microsoft Excel format). Summary of lithological and palynological indicators for the depositional environment interpretation of the 105-AM well.
- table S9 (Microsoft Excel format). LOC data points for Saltarin versus composite, 105-AM versus composite, and 105-AM versus Saltarin.
- table S10 (Microsoft Excel format). Age of individual samples derived from the graphic correlation analysis.
- table S11 (Microsoft Excel format). Total carbon, total inorganic carbon, total organic carbon, total nitrogen, and carbon isotope data for all studied samples.
- table S12 (Microsoft Excel format). Mollusks identified in core 105-AM.

section S1. General information

In the following pages we describe in detail all the different techniques used in this study together with an extensive literature review and expanded results (figs. S1 to S19, tables S1 to S12, and online files S1 to S6).

1. 1 Summary of previous studies in Western Amazonia

Western Amazonia is a vast territory, ~3,500,000 km^2, about half the area of the continental United States. It is covered mostly by tropical rainforest. Outcrops are scarce and they are found generally as 3 to 60 meter-thick exposures along river margins that often are accessible only during the dry season when river levels are down. Outcrops nevertheless provide invaluable information on lateral facies changes and give a 3-dimensional representation of vertical and lateral variations of lithofacies and depositional environments. Furthermore, access to the region is very limited as there are very few roads thus rivers are generally the only transportation pathway.

The Neogene of Western Amazonia has been the subject of numerous studies over the past 30 years, including palynology (*17, 21-23, 36, 65*), sedimentology/stratigraphy (*10, 12, 13, 18, 20, 24, 25, 28, 66-78*), invertebrates (*13, 26, 71, 79-94*), vertebrates (*15, 95-103*), and isotopes (*29, 104-106*).

There are several structural basins in Western Amazonia including Amazonas/Solimões, Putumayo, Oriente, Napo, Pastaza/Marañon, Acre, Ucayali, and Madre de Dios (*21, 34, 107-110*) (fig. S1). Our study is limited to the northernmost basin, the Amazonas/Solimões Basin, which bounds to the north with the Llanos Basin of eastern Colombia, also included in this study. The Amazonas/Solimões Basin is separated from the Llanos Basin by the Vaupés Arch (fig. S1).

1.2 General Geology of the Llanos Basin

The Llanos Basin has been a foreland basin since the late Eocene, when rapid accumulation initiated especially close to the present-day Llanos Foothills (*53, 111-116*), which correspond to the eastern border of the Andes. The thickness of the foreland strata varies from 4500 meters in the Llanos foothills (proximal foredeep) to 600 meters toward the eastern Llanos (distal foredeep) (*54, 112*). Upper Miocene foreland strata accumulation extended eastward ~500 km from the Llanos foothills according to deep-well correlations and geodynamic models (*52, 117-119*).

There are few published studies of Miocene stratigraphy and depositional environments in the distal Llanos Basin, as the extensive history of oil exploration in the basin concentrates mostly in Oligocene and older strata in the proximal Llanos Basin (Llanos foothills; e.g., (*116, 120*)). The Cenozoic stratigraphic history of the basin has been divided into several tectono-stratigraphic sequences. Proximal foredeep strata of the Oligocene–lower Miocene belongs to the upper Carbonera Formation, and accumulated along the eastern flank of the Eastern Cordillera (*112, 114*). This tectonic sequence is characterized by alternation of muddy and sandy deposits, with localized conglomerates close the active thrust faults (*114*), and a wedge-like geometry of foreland deposits thickening westward. Fine-grained strata include (1) laminated dark-gray mudstones with

thin coal seams and bioturbated fine-grained sandstone, and (2) laminated mudstones with mollusks and marine-brackish-water indicators aggrading to tabular and wavy laminated, locally bioturbated, fine-grained sandstones (*53, 112, 114*). Coeval strata in the distal foredeep consist of amalgamated sandstones (*54, 117*). The overall pattern suggests a fluvial-deltaic plain in the proximal foredeep developing into a flood plain and a coeval lacustrine-lagoonal depositional system in the middle foredeep and a fluvial-dominated system derived from the craton in the distal foredeep (*52-54, 112*). A short-lived marine flooding event in the early Miocene has already been documented in the Llanos foothills (*121*).

Middle and upper Miocene-Pliocene strata belong to the Leon and Guayabo formations, respectively, and form of the youngest tectonosequence. The Leon Formation is characterized by dark-colored laminated mudstones and shales with isolated records of mollusks and foraminifera; sandstone content increases northward and westward (*111, 116, 117, 120*). Overlying this unit is the upper Miocene-Pliocene Guayabo Formation, which consists of upward-coarsening deposits that become thicker and coarser toward the Andean deformation front (*114*). This unit is also characterized by beds of varicolored mudstones and lithic sandstones, suggesting fully fluvial and alluvial-fan environments supplied by the growth of the Eastern Cordillera to the east and the Vaupés Arch to the south (*34, 52, 54, 112*).

The Saltarin well is located in the distal foredeep basin and it has a complete record of the two tectonosequences described above. Geodynamic analysis of the Oligocene–present Llanos foreland basins indicate that (1) along-strike differences of orogen growth patterns play a primary role in the geometry and location of the foredeep and forebulge depozones, (2) the forebulge is buried during most of the two tectonosequences, and (3) tectonic subsidence related to vertical forces due to mantle flow explains a broader long-wave geometry of the Llanos Basin during the Miocene compared to the Oligocene (*11, 117*), mainly for the distal Llanos Basin.

1.3 General Geology of the Amazonas/Solimões Basin

The Solimões Basin is an intracratonic sag basin that covers northern Brazil, southern Colombia and the border region of adjacent Peru (fig. S1) (*122, 123*). This basin is bounded to the north and south by the Guiana and Brazilian Shields, respectively, which are composed mainly of Precambrian rocks (fig. S1). At the north of the Solimões Basin is the Colombian Amazonas Basin, a northwest-striking intracratonic basin. The Amazonas Basin is separated from the Llanos Basin by the Vaupés Arch to the north, and from subandean Putumayo Basin by the Chiribiquete Arch to the west (fig. S1) (*123*).

The Amazonas/Solimões Basin is filled with a Oligocene-Miocene succession up to 1.5 km thick (*124*). This succession is composed of continental floodplain, lake and swamp deposits of the Ramon and Solimões formations (*122-124*), with some evidence of marine ingressions (see references in 1.1 Summary of previous studies in Western Amazonia). Coupling of Andean deformation and Pacific subduction processes during the Miocene caused both the regional tectonic subsidence and local reactivation of

Precambrian structures that form the present Vaupés Arch (*11, 34*) in the Colombian Amazonas-Vaupés basin.

section S2. Sedimentology and sequence stratigraphy analyses

2.1 Location and nature of the wells

Saltarin (the official name is Saltarin 1A) is a well drilled by Hocol S.A. in 2008 and it is located in the distal Llanos Basin of Colombia (4.612º N, 70.495º W) (fig. S2, table S5). This is a well drilled almost perpendicular to horizontal strata, and cored from 4 to 671 meters below surface. Only a total of 19 meters (5.12%) were not recovered. This well was described and analyzed for stratigraphic and provenance studies in 2008 (*54*), and the core is preserved at the National Core Library in Bucaramanga, Colombia. Edward Duarte and Germán Bayona made a revision of the sedimentological and stratigraphic analysis in 2015, using the input of new biostratigraphic data presented in this manuscript (fig. S3).

The well 105-AM (official name is 1-AS-105-AM) was drilled by the Geological Survey of Brazil in 1976 (*125*), and it is located in the Amazonas/Solimões Basin in northwestern Brazil (4.25º S, 69.93º W) (fig. S2, table S5). This well cored a total of 405 meters. Vladimir Zapata and Carlos D'Apolito made the core description. Edward Duarte and Germán Bayona carried out the sedimentological and stratigraphic analysis using the composite log, the core description and the new biostratigraphic data presented in this manuscript (fig. S8).

2.2 Extended Methods

Saltarin and 105-AM cores were described at a scale of 1:50 for identification of grain-size trends, sedimentary structures, clast composition, thickness of lamination, bioturbation patterns, and macrofossil identification, all of which are used to identify individual lithofacies. The association of lithofacies within a vertical and conformable succession supports the interpretation of depositional environment, following the criteria in James and Dalrymple (*38*) and Miall (*39*). Sequence stratigraphy analysis follows the criteria described in (*40*) for definition of dominant stacking patterns of deposition (aggradation, progradation and retrogradation) and bounding surfaces (sequence boundaries, maximum flooding surfaces) that may be used for regional correlation. For fluvial strata, we used the terms "low accommodation" and "high accommodation" system tracts, as discussed in (*40*). For homogeneous fine-grained strata accumulated in shallow waters, we used a combination of lithofacies and biostratigraphy data to identify the stratigraphic surfaces of correlation. All sedimentological, biostratigraphic and stratigraphic data are stored and displayed using SDAR software (*41*). Stratigraphic columns are presented here at a scale of 1:1000.

We grouped depositional settings intro three major depositional environments: Continental, Marginal and Marine. (1) The Continental environment includes interbeds of massive to cross-bedded sandstones and conglomeratic sandstones with a sharp lower contact and light-colored mudstones that can contain sideritic spherulites and nodules. These lithofacies represent accumulation in fluvial channels and adjacent floodplains with evidence of paleosol development by subaerial exposure. (2) The Marginal

environment includes greenish to gray-colored, laminated, bioturbated, and locally fossil-rich mudstones coarsening up to very fine to medium-grained sandstones with coal interbeds. The association of these lithofacies represents accumulation on deltaic plains, low-energy wetlands with swamps, ponds and channels, and shallow fresh-water lacustrine systems. (3) The Marine environment includes planar-laminated and massive fine-grained lithofacies. In 105-AM, marine lithofacies also include organic matter (peat) and fossil fragments. The content of both marine palynomorphs (dinoflagellates, marine acritarchs, foram linings) and macrofossils in those lithofacies supports the marine environment interpretation, yet salinities may have been in part very low.

2.3 Sedimentology and sequence stratigraphy of the Saltarin well

The Saltarin well was drilled into three stratigraphic units, named from top to base as Guayabo, Leon, and Carbonera (not drilled completely) formations (fig. S3). The drilled portion of the Carbonera Formation includes a lower member (16.4 m; unit C3, Carbonera units after (*111*)) of interbedded subarkose sandstones, coal, and massive kaolinite claystones with siderite spherules. This association represents accumulation in fluvial channels and adjacent floodplains with paleosol development. This unit changes gradually upwards to greenish laminated and locally bioturbated mudstones of the middle member (46.4 m; unit C2) that record the lower marine interval. Overlying the middle member in a sharp unconformable contact are cross-bedded to massive conglomeratic sandstones (quartzarenites and subarkoses) grading to medium/fine-grained sandstones of the upper member (61.3 m; unit C1), which accumulated in a fluvial system. The Leon Formation (105.1 m thick) is identified as homogenous greenish laminated to massive mudstones that contains the second marine interval. The contact with the overlying Guayabo Formation (441.8 m) is gradual, and this unit was divided into six informal members, named from base to top as G1 to G6 (*54*). G1 (53.8 m) consists of upward-coarsening mudstones to fine-grained subarkoses passing up-section to dominantly mud-dominated (G2, 75.1 m) and then to an interval of feldspathic litharenite (G3, 41.4 m) units with abundant siderite spherules. The lower three members record the advance of deltaic plains and establishment of continental fluvial plains to the top. G4 (66 m) is another mud-dominated interval with intense bioturbation in some segments as well as preservation of lamination and thin sandstones interbeds in other segments. G5 (123.9 m) is a sand-dominated interval, internally massive, cross-bedded and laminated and compositionally identified as feldspathic litharenites. G6 (81.6 m) consists of interbeds of fining-upward quartzarenites and massive mudstones with siderite spherules. The upper three members accumulated in fluvial plains that record both deformation of the Vaupés Arch to the south (G4 and G5 members) and the supply of sediments supplied from the Eastern Cordillera (G6 members) (*54*).

The two marine intervals are recorded in similar greenish laminated mudstones both in the middle member of the Carbonera Formation and in the Leon/member G1 of the Guayabo Formations, and correspond to the retrogradational segment and maximum flooding surfaces of two major sequences (fig. S3). The lower sequence involves the three members of the Carbonera Formation that record the retrogradation from a fluvial to marginal-lacustrine system, and prograding abruptly to a fluvial system to the top. The upper sequence records the flooding of the fluvial-deltaic system in the lower Leon

Formation, passing to an aggradational accumulation of a lacustrine-marine system in the middle and upper Leon Formation, and then passing upsection to the gradual progradation of deltaic and fluvial plains of the Guayabo Formation (fig. S3). Summaries of lithological associations, depositional environment interpretation, and stacking patterns of stratigraphic sequences identified from meters 300 to 671 (lower members of the Guayabo, Leon and Carbonera formations) are found in table S7 and fig. S3 with emphasis in the two marine intervals documented in this study. A more detailed and complete description and interpretation of this well, including meters 4 to 300, is provided by (*54*).

2.4 Sedimentology and sequence stratigraphy of 105-AM well

Well 105-AM drilled the Solimões (26.2 to 332.7 m) and Ramón formations (332.7-405 m). Three informal members were identified within the Solimões Formation (fig. S8):

-The lower member (332.7 – 267.5 m) includes three sequences that consist of very thick beds of massive to laminated claystones, siltstones and carbonaceous siltstones passing upsection to medium to thick bedded sublitharenites, locally with cross beds, and thin to medium beds of lignite. A similar succession is documented for the uppermost sequence for the Ramón Formation (358.8- 332.7), but the Ramón arenites are quartzose in composition.

-The middle member (168.2-267.5 m) includes two very thick sequences characterized by three lithofacies associations, that from base to top are: (1) laminated and carbonaceous siltstones with fossil fragments in the upper sequence; (2) siltstones interbedded with decimeter- to meter-scale lignite beds; and (3) lithic-bearing, upward fining and coarsening sandstones with oxides and sideritic-rich beds product of paleosol development. We interpret that the lower interval corresponds to the retrogradational segment of the sequence, whereas the second and third interval correspond to the aggradational to progradational segment of the sequence.

-The upper member (26.2-168.2 m) includes five sequences whose lower retrogradational segment includes gastropods, bivalves, and other shell fragments in fine-grained laminated, bioturbated to massive siliciclastic strata and biomicrites that pass upsection to upward-fining sublitharenites with thin to medium beds of lignite; the fossil content decreases upsection, with simultaneous thickening of sandstone interbeds. The molluscan fauna represents endemic long-lived lake settings.

The two marine intervals are recorded in claystones with organic matter and thin oxidized sandstone interbeds of the lower member (284-293.3 m) and in mollusk-rich carbonaceous siltstones of the upper member (101.4 to 96.7 m) (table S8). These marine intervals correspond to the retrogradational segment and maximum flooding surfaces of two major sequences. The lower sequence involves the lower and middle member of the Solimões Formation that accumulated mainly in the environment we refer here as Marginal that includes low-energy wetlands with dominance of swamps that allowed the preservation of organic material and development of lignite passing laterally to ponds and subaerial floodplains (forming paleosols) crossed by fluvial channels (fig. S8). The upper sequence accumulated under more oxygen-rich lake floors systems that facilitated

preservation of the gastropod and bivalve fossil record. Both sequences record thin fluvial intervals in their top.
The variation of lithological associations in both marine intervals of 105-AM, the short periods of subaerial exposure to develop paleosols in the lower marine interval, as well as the lower proportion of marine palynomorphs in both intervals compared to the proportions in Saltarin, indicates that the marine environment of 105-AM is much more shallower and less saline that the marine intervals in Saltarin (table S8).

A summary of lithology associations, depositional environment interpretation and stacking patterns of stratigraphic sequences identified in the Ramón and Solimões formations are in table S8 and fig. S8 from meters 26.2 to 358.8, with emphasis on the two marine intervals documented in this study.

section S3. Marine intervals

3.1 Palynology

3.1.1 Marine Intervals Saltarin

A total of 30,138 palynomorphs representing 493 taxa, were counted in 138 samples (about one sample per 4.7 stratigraphic meters) from the Saltarin core (table S1). The Saltarin core has two stratigraphic intervals with a significantly higher proportion of marine palynomorphs, intervals 645.6 m to 617.6 m and 548 m to 408.4 m (table S3). Mean percentage of marine palynomorphs in interval 645.6 m to 617.6 m is 24.3% while mean percentage of marine palynomorphs in interval 548 m to 408.4 m is 39.6%. In contrast, mean percentage of marine palynomorphs in interval > 645.6 m is 2.7%, interval 617.59 to 548.1 m is 3.9%, and <408.4 m is 0.9% (table S3). Percentage of marine palynomorphs of both marine intervals is significantly higher that non-marine intervals (t-test, $p < 0.01$, DF = 53.2).

The proportion of lacustrine palynomorphs varies little among the five intervals (table S3), most of differences not being significant, *t-test* >645.6 (0.1%) vs. 645.6-617.6 (1.9%), p=0.02, df=16.1; 645.6-617.6 (1.9%)vs. 617.59 to 548.1 (4%), p=0.5, df=12.4; 617.59 to 548.1 (4%) vs. 548-408.4 (4.4%), p=0.9, df=15.3; 548-408.4 (4.4%) vs. <408.4 (3.3 %), p=0.5, df=59.9.

3.1.2 Marine Intervals 105-AM

A total of 23,640 palynomorphs of 428 taxa, from 95 samples (about one sample per 3 stratigraphic meters), were counted in the core from 105-AM (table S2).

The 105-AM core has also two stratigraphic intervals with a significantly higher proportion of marine palynomorphs: interval 293.3 to 284 m and interval 101.4 to 96.7 m (table S3). Mean percentage of marine palynomorphs in former interval is 33.8% and in the latter is 16.3%. In contrast, mean percentage of marine palynomorphs in interval > 293.3 m is 2.4%, interval 283.9 to 101.5 m is 0.1%, and <96.7 m is 0.1% (table S3). Percentage of marine palynomorphs of both marine intervals is significantly higher that non-marine intervals (t-test, $p < 0.04$, DF = 7). There is a single sample at meter 326.2 that has a 25.6% abundance of marine palynomorphs. Samples in close stratigraphic

proximity above (meters 324.9, 325.1, 325.3) and below (meters 327.0 and 332.3) lack marine palynomorphs. The marine palynomorph elements at sample at 362.2 consist only of chitinous foram linings and do not contain dinoflagellates. Foram linings can be abundant in tidal settings and are probably carried occasionally into nearby plains by large storms. The lack of dinoflagellate cysts together with the lithological characteristic of the stratigraphic interval (light brown mudstone with sporadic organic matter and coal) suggests a Marginal environment rather than a shallow marine platform for sample 326.2 m and nearby samples above and below.

Differences in the proportion of lacustrine palynomorphs among the five intervals are mostly insignificant (table S3): *t-test* >293.3 (3.3%) vs. 293.3-284 (0.2%), p=0.1, df=11; 293.3-284 (0.2%)vs. 283.9-101.5 (2%), p=0.04, df=35.8; 283.9-101.5 (2%) vs. 101.4-96.7 (5.5%), p=0.26, df=4.8; 101.4-96.7 (5.5%) vs. <96.7 (7.9 %), p=0.75, df=10.1.

3.1.3 Dinoflagellate cysts and acritarchs

The marine palynomorph assemblage in Saltarin contains eight species of dinoflagellates/acritarchs in the lower interval and 25 species in the upper interval (table S1). The marine palynomorph assemblage in 105-AM contains 15 species of dinoflagellates and acritarchs in the lower interval and ten species in the upper interval (table S2). The preservation is moderate to poor. Many specimens are torn or folded with broken processes. Reworked pre-Neogene dinoflagellate cysts are recorded. The lowest marine interval in 105-AM (table S2) records the presence of the dinoflagellate cyst species *Apteodinium*? *vescum*, *Cleistosphaeridium ancyreum*, *Cleistosphaeridium placacanthum, Quadrina* "incerta" (=Dinocyst XI of (*126*)) and the acritarch *Quadrina*? *condita.* The upper marine interval contains *Lingulodinium machaerophorum, Operculodinium israelianum, Quadrina*? *condita, Spiniferites, Trinovantedinium ferugnomatum*, and *Tuberculodinium vancampoae* (fig. S5).

The marine intervals in Saltarin contain *Q.*? *condita*, *Trinovantedinium papula* and *T.*? *xylochoporum* among many other species (table S1, fig. S3).

Most of the dinoflagellate cysts from both marine intervals in 105-AM are neritic, cosmopolitan species with a broad temperature tolerance. No characteristic oceanic species are present. Only *Operculodinium israelianum* and *Tuberculodinium vancampoae*, present in both marine intervals, have a restricted temperature range and occur in the subtropical, tropical and equatorial realm, favoring nearshore sites or very shallow areas, respectively (*127*). Highest relative abundances for *T. vancampoae* are recorded when sea surface salinities are higher than 32.9 psu (*127*). The upper marine interval holds also high relative numbers of *Lingulodinium machaerophorum*, an euryhaline species often occurring in higher numbers in estuarine environments, or in areas with diffuse very shallow upwelling (*128*). *Operculodinium israelianum* and *T. vancampoae* in the upper marine interval of Saltarin also suggest deposition in low-latitude shallow waters, corroborated by presence of the very shallow to fully marine *Polysphaeridium subtile* (*127*).

Species of the genera *Erymnodinium*, *Selenopemphix*, *Sumatradinium* and *Trinovantedinium*, together with round brown cysts of unspecified protoperidiniacean affinity, are distinctly present, albeit in a varying degree, in the marine intervals of both cores. These are dinoflagellate cysts of the Family Protoperidiniaceae, which are essentially nonphotosynthetic or heterotrophic dinoflagellates (*129*). Protoperidiniacean cysts are sensitive to post-depositional degradation through oxidation (*130*). The occurrence of large numbers of heterotrophic cysts in shelfal environments is related to enhanced nutrient levels through upwelling or fluvial/deltaic input (*128*). Protoperidiniacean-dominated dinocyst assemblages are documented from the Oligocene of Nigeria (*131*) and the Miocene of the Gulf of Mexico, off Louisiana (*132*), where enhanced nutrient input was delivered in the depositional area by the Niger Delta and Mississippi delta complex, respectively.

3.2 Branched vs. isoprenoidal tetraether (BIT) index

Organic compounds were extracted from powdered and freeze- dried sediments with dichloromethane (DCM)/ methanol (MeOH) (9:1, v/v) by using the accelerated solvent extraction technique (Dionex). Excess solvent was removed using a rotary evaporation with vacuum. The total extracts were separated into polar and apolar fractions over an activated Al_2O_3 column using hexane:DCM (1:1, v/v) and DCM:MeOH (1:1, v/v), respectively. The polar fraction was then dissolved in a 99:1 (v/v) hexane/isopropanol mixture, and sieved using a 0.45 μm, 4 mm diameter polytetrafluoroethylene (PTFE) filter, before being analyzed using a high-performance liquid chromatography/atmospheric pressure positive ion chemical ionization mass spectrometer (HPLC/ APCI-MS). HPLC/APCI-MS analyses were done according to Schouten et al. (*49*) using an Agilent 1100 series LC/MSD SL and separation and a Prevail Cyano column (2.1 × 150 mm, 3 mm; Alltech), maintained at 30 °C. The GDGTs were eluted using a changing mixture of hexane and isopropanol as follows: 99% hexane to 1% propanol for 5 minutes, then a linear gradient to 1.8% isopropanol for 45 minutes. Flow rate was 0.2 ml per minute. Single ion monitoring was set to scan the 8 $[M+H]+$ ions of the GDGTs with a dwell time of 237 ms for each ion.

The lower interval has an average BIT of 0.16 (N=5) and the upper interval has a BIT of 0.30 (N=13) (table S4), indicating a low contribution of soil-derived tetraether lipids for both intervals, and typical for shallow marine sections (*30*).

3.3. Marine macrofossils

3.3.1 Carcharhiniformes gen. et sp. indet.

Systematics

Neoselachii Compagno 1977

Galeomorphii Compagno 1973

Carcharhiniformes gen. et sp. indet. (Carcharhinidae or Sphyrnidae) (fig. S6)

Material Examined.—Specimen MUN STRI-40967, Mapuka Museum of Universidad del Norte, Barranquilla–Colombia, Saltarin Core, meter 630.08, Carbonera C2 Formation, early Miocene.

Description.—Specimen is a lateral tooth. The tooth is not complete (~ size: width 7.75 mm and height 6.13 mm), and it has a high, triangular, asymmetric, broad and distally

inclined crown, broken at the apex. The lingual face is strongly convex and the labial one is flat. The mesial cutting edge is convex, and there is no clear differentiation between this and the mesial heel. The distal cutting edge is straight in the base and slightly concave in its upper part. Both cutting edges are strongly serrated. The distal heel is distinctive and serrated, and well separated from the cusp by a shallow notch. The preserved root is low with the basal surface slightly concave and is missing the distal lobe. The lingual protuberance is not well preserved.

Remarks. This tooth might belong to *Carcharhinu*s (Carcharhinidae), however, a strongly serrated cusp and a distinct distal heel with a shallow notch are features also present in teeth of the extant Great Hammerhead, *Sphyrna mokarran* (Sphyrnidae). The latter species is the only sphyrnid with teeth with strongly serrated crowns (*133, 134*). Due to the existence of only one specimen, which lacks more diagnostic characters (e.g. a complete root and lingual protuberance), we refrain from assigning it to a more precise taxonomic level. Extant *Carcharhinus* and *Sphyrna* species are common inhabitants of marine environments, although some species can tolerate low salinity levels (brackish environments) (*32*). Only the Bull shark *Carcharhinus leucas* is known to going long distances into rivers (*32*), however, the tooth found is not referable to *Carcharhinus leucas*.

3.3.2 Squillidae

Systematics

Phylum Arthropoda von Siebold, 1848 (*135*)
Class Malacostraca Latreille, 1802 (*136*)
Order Stomatopoda Latreille, 1817 (*137*)
Family Squillidae Latreille, 1802 (*136*)

Material Examined.—Specimen MUN STRI-40281, Mapuka Museum of Universidad del Norte, Barranquilla–Colombia, Saltarin Core, meter 636, Carbonera C2 Formation, early Miocene (fig. S7).

Description.—Dactylus of second thoracopod armed with seven sharp, slender and curved spines on occlusal surface, heavily ornamented with minute barbed bands. The first spine is half the total dactylus length, measured from distal margin to proximal portion. Second to fourth occlusal spines are broken. Fifth to seventh spines very well preserved; fifth spine one-sixth the dactylus maximum length, and one-third as long as first spine; sixth spine one-fourth as long as first spine; seventh spine the smallest, one-sixth the first tooth length. Spines bearing a narrow carina on their dorsal margin. Outer margin of dactylus lacking prominent angular projections (fig. S7).

Remarks. Stomatopods, also known as mantis shrimps, are aggressive ambush predators that can be grouped by the morphology of their raptorial appendages, or second thoracopods, which they use to either crush hard shelled invertebrates (‘smashers’) or impale soft-bodied prey (‘spearers’) (*33*). The stomatopod remains recovered from the Miocene Carbonera Formation are referable to the ‘spearer’ family Squillidae due to the overall shape, number of spines, and barbed tip ornamentation of the dactyl of the second thoracopod. Similar fossils from the Pliocene of North Carolina assigned to the genus *Squilla* (*138*) show similar anatomical traits to those present in the new material, such as the presence of multiple barbed spines that bear a narrow carina on their dorsal margin (fig. S7). Squillids are marine-restricted stomatopods that dwell in burrows in soft,

muddy to sandy sediments, of tropical and subtropical low intertidal to shallow subtidal habitats (*33, 139, 140*). The occurrence of squillid mantis shrimp remains in the Carbonera Formation confirms the presence of shallow marine settings in the Llanos Basin during the early Miocene, and indicates that marine, ambush predatory crustaceans were conspicuous elements of the paleo-ecological association herein described.

section S4. Basin-wide correlations

4.1 Seismic and well Interpretation

4.1.1 Extended Location and methods

A total of 1148 km of 2D seismic lines were selected in order to correlate the two intervals of marine incursions in the Llanos Basin with the intervals of marine incursions in the Amazonas/Solimões Basin (early Miocene marine incursion (EMI) and the middle Miocene marine incursion (MMI)) (fig. S2, table S6). Seismic lines selected in the distal Llanos basin cover the area between the Saltarin well and the northernmost expression of the Vaupés Arch in the subsurface (fig. S13). These seismic lines are analyzed in conjunction with the electric logs of nine wells (fig. S9). In the Amazonas/Solimões Basin, a few seismic lines along major rivers in Colombia and a published seismic line in Brazil (*37*) allowed us to compare seismic facies between the two basins (figs. S2 and S14); however, there are no wells near those seismic lines that would permit a better integration of seismic facies with stratigraphic units (fig. S14). A total of nine isolated outcrops of Miocene units along river margins, as well as 2 cores in Solimões Basin, are the only reference for identification of the uppermost seismic level (figs. S2, S14 and table S5).

4.1.2 Results for the Llanos Basin

Three seismic horizons were mapped in the distal Llanos basin (fig. S13), which can be characterized from base to top as:

(1) A strong and laterally continuous peak that represents the top of the Carbonera Formation. Parallel and continuous seismic reflectors below that contact and an interval of low-amplitude peak and troughs, which is also parallel to the top of the Carbonera Formation, correspond to the sandy-dominant C1 and shale-dominant C2 units. The tabular and parallel geometry characterizes the C2 unit. In contrast, non-parallel and discontinuous reflectors characterize the underlying units of the Carbonera Formation.

(2) The shale-dominant Leon Formation is characterized by a thick homogeneous interval of low-amplitude peak and troughs. However, this seismic facies changes laterally to seismic reflectors with moderate-amplitude peak and troughs above the Vaupés Arch (fig. S13).

(3) The lower members G1 and G2 of the Guayabo Formation are characterized by the presence of high-amplitude peaks and troughs, which are more laterally continuous at the base and more discontinuous upsection.

Electric logs of the analyzed wells are mainly gamma ray profiles, which were used to make two stratigraphic correlations to integrate palynological, sedimentological and

sequence stratigraphic analyses carried out in the Saltarin well with other nine wells. Three wells (E, F, H in fig. S9) have reported age control and indicators of marine influence (*53*). The northern correlation, with a length of 200 km, correlates the Saltarin and other five wells following an orientation parallel to the eastern margin of the distal Llanos Basin. The southern correlation, with a length of 90 km, correlates wells in the depocenter of the distal Llanos Basin with wells located in the northernmost expression of the Vaupés Arch (fig. S9).

Analyzed stratigraphic units have the following electric log pattern (electrofacies):

(1) A funnel-like and serrate geometry for the C1 and C2 Carbonera units, with gamma values decreasing upsection due to the change from mud-dominant to sandy-dominant units.

(2) A cylinder and serrate geometry for the Leon Formation, as the high gamma ray values keep constant due to the homogeneous mud-dominant lithology.

(3) A funnel-like and serrate geometry for the lower members G1 and G2 of the Guayabo Formation due to the upsection increase of sandstone interbeds.

Basement highs observed in the southern segment of the easternmost seismic line (toward the Guiana Shield) and the southernmost seismic line show the subsurface expression of the northern extension of the Vaupés Arch (figs. S2 and S13). These seismic images indicate that the early Miocene marine incursion covered almost all the northern extension of the Vaupés Arch, but it was only the accumulation of the top of the Carbonera Formation that totally covered these basement highs (figs. S9 and S13). The seismic reflector corresponding to the top of the Carbonera Formation is traced in the area that corresponds to the northernmost extension of the Vaupés Arch, but the stratigraphic thickness of the Carbonera and Leon units decreases toward those buried basement highs. Seismic reflectors of the Leon Formation are deformed by the uplift of the Vaupés Arch in late Miocene time, as indicated by (*34*).

The seismic horizon corresponding to the Leon Formation can be traced southward. The thickness of this stratigraphic unit increases to the depocenter of the distal Llanos Basin in both correlations (wells F and G), and the dominant lithology is mudstones (fig. S9). However, the lower Leon Formation and the C2 unit of the Carbonera Formation change gradually to sandy units in the southernmost well of the southern correlation (well I in fig. S9). This well is the closest to a basement high in the northernmost Vaupés Arch. The upper segment of the Leon Formation, which records the maximum extension of the middle Miocene marine incursion in the Llanos and Amazonas/Solimões Basins, corresponds to the thin muddy interval that covers the sandy unit in the southernmost well of the southern correlation (well I in fig. S9).

4.1.3 Results for the Amazonas/Solimões Basin

Seismic information for Cenozoic units in the Amazonas/Solimões Basin, which corresponds to the shallowest segment of the seismic profile, has very poor resolution because the seismic acquisition is designed to image deeper strata of Paleozoic age. Seismic facies of Cenozoic units in the Amazonas/Solimões Basin are very different from those identified in the Llanos Basin, reflecting the contrasting lithological associations of Miocene units in both basins, as described with detail in cores (figs. S3 and S8). The lowest 400 m of the analyzed seismic images (fig. S14), which corresponds to the Oligocene and Miocene strata, show parallel, moderately continuous and horizontal seismic horizons with high-amplitude peaks and troughs; however, the amplitude of the peaks and troughs varies laterally. Minor discontinuities of these reflectors may be a product of local faults.

Seismic lines in the Vaupés Arch and the Amazonas Basin in Colombia show undifferentiated Oligocene and Miocene units over Paleozoic strata. The structure of Oligocene and Miocene units is almost horizontal, but they are cut by vertical faults (fig. S14). These faults are more prominent in the Vaupés Arch, and late Miocene deformation causes the erosion of Neogene strata in the Vaupés Arch (*34, 123*), eroding the connection between the Llanos and the Amazonas basins.

Nine Miocene outcrops in northern Amazonas with palynological control, depositional environment interpretation, and evidence of marine incursions (*17, 23, 36*) were reinterpreted using the biozones proposed in (*56*) to determine which of the two marine incursions they correlate with. Three sections record an early Miocene incursion (top of T12 and base of T13 biozones), whereas the other six sections record the middle Miocene incursion (top of T-14 and T-15 biozones) (fig. S10). The information of wells 4a-AM (*21*) and 105-AM (this study) complement the dataset of information to document the Miocene incursions in the northern Amazonas/Solimões Basin (fig. S10). The three northernmost sections show the earlier entrance and later retreat of the early Miocene marine incursion than in wells 4a-AM and 105-AM. Also, this correlation shows a nearby connection with continental settings of the Guiana Shield (see A – A´ correlation in fig. S10). A similar pattern occurred in the middle Miocene marine incursion, with an earlier record in the north (Apaporis IV section) compared to south (five sections and two wells, see B – B´ correlation in fig. S10). Continental environments are only recorded in the southernmost sections (wells 4a-AM and 105-AM), suggesting that in late middle Miocene the source areas retreated southeastward relative to the position of the early Miocene incursion.

4.2 Paleogeographic reconstruction

The paleogeographic reconstruction records the changes in depositional trends in map view (regression and transgression) as a result of the two marine incursion intervals in the Llanos and Amazonas/Solimões basins. The extent of deposition was limited and strongly controlled by two major structural features that supplied sediments to the basin: (1) the Northern Andes deformation front to the west and (2) the depositional boundary along the Guiana Shield to the east. A third structural feature is the position of intrabasinal uplifts (Macarena range, Vaupés Arch and Baúl High, see fig. S1), which controlled

locally the orientation of marine incursions and supplied sediments to the surrounding basins. The northern boundary of our reconstruction is the Eastern Venezuela Basin (fig. S1), where continuous marine sedimentation took place during the early and middle Miocene (turbiditic deposits of the Carapita Formation (*141*)). This unit changes southward (to the Guiana Shield) from shallow marine to continental deposits of the Oficina and Merecure formations (*141*). This basin is bounded to the north by the tectonic growth of the accreted Serranías (not shown in the maps for simplicity), the growth of the Baúl High in the middle Miocene, and the initial uplift of the Merida Andes dating to the Oligocene (*142*). Oligocene marine incursions that affected the Barinas-Apure-Llanos basins also had connection with the Eastern Venezuela Basin (*53, 143*).

Marginal and Continental depositional environments dominated siliciclastic accumulation in the Llanos and Amazonas/Solimões basins at the Oligocene-Miocene boundary (*53, 112*). Terrigenous detritus derived from the northern Andes uplifts (Eastern Cordillera and Merida Andes) and the Guiana Shield were transported by fluvial systems to an axial Marginal system, which was connected to the Caribbean Sea in the Eastern Venezuela basin, as described above. The distribution of *Pachydon hettneri* in the Amazonian, Llanos, Magdalena and Eastern Venezuela basins shows biogeographic continuity and exchange during the early Miocene (*87*).

Tectonic subsidence and global rise of sea level in the early Miocene created accommodation space that overwhelmed the rate of sedimentation, allowing the marine incursions inland (*36*). The combination of these processes resulted in the onset of a rapid transgression at 18.1 Ma that reached the northern Amazonas/Solimões Basin. The early Miocene incursion moved southward along the coastline ~1300 km into the Amazonas/Solimões Basin. This incursion passed through a strait, named here the Caguán Strait, which was generated between the Macarena Range and the depositional boundary along the Guiana Shield. The transgression of the EMI reached its largest extension ca. 17.8 Ma, at least 1650 km southward from the Eastern Venezuela basin, and southward of wells 4a-AM and 105-AM (Fig. 2B). Paleosol development was stronger in 105-AM than in Saltarin, representing more widespread continental conditions in the former that corresponds to shallower marine water depths in both incursion intervals.

In the late early Miocene (~17.8 to ~16.3 Ma.) filling of the subaqueous basin with lake, swamp and fluvial deposits initiated, and marine conditions retreated northward more than 1400 km (Fig. 2E). Amalgamated channel sandstones accumulated in the Llanos Basin, whereas channel-fill and floodplain deposits accumulated in the Amazonas/Solimões Basin. What caused the fall of base level and retreat of the coastline is still a subject that needs further investigation.

At the latest early Miocene (ca. 16.3 Ma) (Fig. 2E) accumulation was strongly influenced by intraplate uplifts, such as the Baúl High and the Vaupés Arch. The former uplift restricted the location of marine deposits farther to the south, relative to the position in the early Miocene (*141*), whereas the latter uplift narrowed the Caguán Strait.

Renewal of structural activity in the northern Andes (*144*) and the increase in the rate of sea level rise in the early middle Miocene (*145*) generated accommodation space, allowing the transgression of the system with marine deposits that corresponded to the middle Miocene Incursion (MMI). The marine incursion extended for more than 1200 km toward the northern Amazonas/Solimões Basin in the earliest middle Miocene (ca. 15.1 Ma) (Fig. 2F). This MMI reached the largest extension during the middle Miocene (ca. 13.7 Ma.), at least 1800 km southward from the Eastern Venezuela Basin, and southward of wells 4a-AM and 105-AM (Fig. 2G). Water depth of the marine incursion was shallower and less saline in 105-AM compared to Saltarin.

In late middle Miocene (ca.12.5-12.6 Ma), the uplift of the Vaupés Arch increased and closed the Caguán Strait (Fig. 2H); therefore, marine incursions continued only in the Llanos Basin, and freshwater accumulation in Marginal settings took place in the Amazonas/Solimões Basin. The increase of sediment supply from the northern Andes together with the onset of global sea-level fall (*145*) caused the northward and eastward retreat of the marine coastline to the easternmost part of the Eastern Venezuela Basin in the early late Miocene (ca. 10.9-10.5 Ma.).

section S5. Chronology of cores

5.1 Zonations for the region

There are several tools for dating strata in the Neogene of the Llanos Basin and Western Amazonia. Palynology has been used over decades in the Llanos Basin as the main chronological tool (*44, 112, 113, 146-149*). The most up-to-date zonation for the basin (*56*) is based on the information of 70 sections and 6707 samples covering the entire Cenozoic. This zonation was calibrated with published information on magnetostratigraphy (*150*), carbon isotopes (*151, 152*), U/Pb (*153*), and foraminifera from the Urumaco Basin (*154-166*).

Tools for dating Neogene strata of Western Amazonia include a zonation based on mollusks using information from tens of short-thickness outcrops and cores (*71, 84*), an ostracod zonation for the middle Miocene using 26 outcrops (*88*), a palynological zonation using one core and tens of outcrops (*21*), mammal chronology (*15, 95, 167*), and two $^{40}Ar/^{39}Ar$ dates from two volcanic ash deposits (*168*).

For this study, we chose to use the palynological zonation of Jaramillo et al. (*56*), as the zonation is robust, palynomorphs are abundant in both cores, and the zonation has already been applied successfully to both the Llanos Basin (e.g., *169, 170*) and the Amazonas/Solimões Basin (*36*).

5.2 Previous dating for Western Amazonia strata

Sediments of the upper Pebas Formation (those sediments outcropping in the river margins in Western Amazonia) have been dated as young as Pleistocene (*16, 171, 172*) in Acre Basin, ages that have been shown to be incorrect (*173, 174*). Some have proposed the existence of a widespread unconformity called Ucayali, which lasted from 15 to 9 Ma and was followed by the deposition of a few meters of upper Miocene to lower Pliocene sediments in all Western Amazon Basins including Madre de Dios Basin (*14, 168*).

Pebas/Solimões also has been dated as late Miocene in Acre Basin (*15, 20, 25*), late early to early late Miocene in Acre and Amazon Basins (*17, 84, 85*); or late Miocene/early Pliocene in Amazonas/Solimões Basin (*65*).

Age and sedimentary environments are not the only controversial aspects of the region. Nomenclature and stratigraphy of the formation(s) outcropping across western Amazonia are very confusing. The terms Pebas, Acre, Solimões, Madre de Dios, Amazonian Tertiary, Mariñame Sand Unit, Ipururu, and Terciario Superior Amazonico are used imprecisely.

Many of the dating and stratigraphic nomenclature discrepancies arise from the extensive nature of the region (~ half of continental USA); the lack of continuous outcrops where a complete Neogene section can be studied; the covering of the landscape by forest; and the paucity of studies given the vast territory to be covered. It is noteworthy that only two cores have been studied (*21, 65*) in the entire area.

Our study has demonstrated that marine intervals in Western Amazonia could be only a few meters thick and are interbedded with tens of meters of non-marine deposits, as previous studies have demonstrated (e.g. *19, 21, 29, 36, 87*). This result underscores the importance of an adequate stratigraphic control along a profile of the entire Neogene sequence. Maia *et al.* (*125*) indicate that the Solimões/Pebas formation can be up to 1100 meters thick south of Iquitos, and most outcrops along river banks expose only 15-20 meters. This lack of continuous outcrops represents a major challenge for understanding the paleogeographic evolution of the Neogene of Western Amazonia. We need many more continuous cores across the Neogene sequence to provide reference points that can tie all outcrops together into a cohesive stratigraphic sequence. Only then can we make progress in solving the landscape evolution of Amazonia.

5.3 Graphic Correlation

It is important to stress that ages provided in this research are relative, and the precision goes as far as the calibration points for the zonation. Ages between calibration points are derived from linear interpolation. Therefore, we do not argue that our ages are precisely calibrated with the geological time record, but they indicate a relative age compared to sediments above and below. These ages represent a hypothesis and it is based on the best information we have at the moment; they could change as more calibration points are added to the zonation or if a calibration point is shifted or the line of correlation of each section is modified. Our ages are fully replicable as we provide the line of correlation, the full zonation, and the calibration points.

5.3.1 Graphic correlation of Saltarin

The line of correlation (LOC) of Saltarin is delimited by several biostratigraphic datums including the first appearance datum (FAD) of *Grimsdalea magnaclavata*, FAD of *Ilexpollenites tropicalis*, FAD of *Striatricolporites poloreticulatus*, last appearance datum (LAD) of *Cyclusphaera scabrata*, FAD of *Cichoreacidites longispinosus*, LAD of *Siltaria dilcheri*, FAD of *Fenestrites spinosus*, and LAD of *Polyadopollenites mariae* (fig. S11, table S9). Useful sequence stratigraphy events are C2-I2, C2-I3H, C1-I1, C1-

I2, L-I2, and L-I8. There are an additional three LOC points, labeled as "correlation with 105-AM" (fig. S11, table S9) that are strictly derived from the correlation between Saltarin and 105-AM (Fig. 1, fig. S15). In other words, there is a break point in the LOC of Saltarin vs. 105-AM, and that break point is extrapolated to the LOC of Saltarin vs. Composite. All the files needed to replicate our analysis in GraphCor are given in Dryad Online File 3. Dryad Online File 4 contains all the events plotted in fig. S11, the correlation of Saltarin vs. Composite.
Composite units corresponding to the depth of each palynological sample were transformed into geological time using the R code of Dryad Online File 2 (table S10). The LOC of Saltarin indicates that the core spans the early to the late Miocene, biostratigraphic zones T-12 *Horniella lunarensis* to zone T 17 *Cyatheacidites annulatus*, 18.5 Ma to 5.5 Ma (Fig. 1, fig. S11). The strata of the Carbonera C3 to C1 Formation span zones T-12 to T13 (18.5 to 16 Ma, early Miocene), the Leon Formation zones T-14 to the base of T-15 (16 Ma to 13.5 Ma, middle Miocene) and Guayabo Formation zones T-15 to T-17 (13.5 to 5.5 Ma, middle Miocene to late Miocene). The lower marine interval, meters 645.6 to 617.6, ranges from zone T-12 to T-13, ~ 18.1 to 17.2 Ma respectively, early Miocene, lasting ~0.9 My (Fig. 1, fig. S11). The upper marine interval, meters 548 to 408.4, extends from zone T13 to T16, 16.1 to 12.4 Ma respectively, middle Miocene, spanning ~3.7 My (Fig. 1, fig. S11).

5.3.2 Graphic Correlation of 105-AM
The LOC of 105-AM is delimited by several biostratigraphic datums including the FAD of *Grimsdalea magnaclavata*, FAD of *Ilexpollenites tropicalis,* FAD of *Bombacadites baculatus,* FAD of *Tuberculodinium vancampoae,* FAD of *Cichoreacidites longispinosus,* FAD of *Retitricolporites crassicostatus*, FAD of *Fenestrites spinosus*, LAD of *Echidiporites barbeitoensis*, and LAD of *Psilastephanoporites herngreenii* (fig. S12, table S9). Useful sequence stratigraphy events are C2-I2, C2-I3H, C1-I1, C1-I2, L-I2, and L-I5. There are an additional three LOC points, labeled as "correlation with Saltarin" (fig. S12, table S9) that are strictly derived from the correlation between Saltarin and 105-AM (Fig. 1). All the files needed to replicate our analysis in GraphCor are given in Dryad Online File 3. Dryad Online File 4 contains all the events plotted in fig. S12, the correlation of 105-AM vs. Composite.

Composite units corresponding to the depth of each palynological sample were transformed into geological time using the R code of Dryad Online File 2 (table S10). The graphic correlation of 105-AM indicates that the core spans the early to the late Miocene, biostratigraphic zones T-12 *Horniella lunarensis* to zone T-16 *Fenestrites spinosus*, 18.8 Ma to 10.7 Ma, (Fig. 1, fig. S12). The strata of the Solimões Formation span from zones T-12 to T-16, (18. 4 to 10.7 Ma, early to middle Miocene). The lower marine interval, meters 293.3 to 284, lies within zone T-12, ~ 18.0 to 17.8 Ma, early Miocene, lasting ~ 0.2 My (Fig. 1, fig. S12). The upper marine interval, meters 101.4 to 96.7, lies within zone T-15, 14.1 to 13.7 Ma, middle Miocene, lasting ~ 0.4 My (Fig. 1, fig. S12).

5.4 Dinocyst biostratigraphy

Biostratigraphical analysis with dinoflagellate cysts and acritarchs supports the age determinations produced by the graphic correlation analysis. The lower marine interval in 105-AM was accumulated at some point during the late Burdigalian to early Serravallian whereas the upper marine interval was accumulated at some point between the late Burdigalian to Serravallian. The lower marine interval in Saltarin was accumulated at some point during the late Burdigalian to Tortonian and the upper marine interval was accumulated at some point from the Langhian to Tortonian.

The lowest marine interval in 105-AM (table S2) contains the dinoflagellate cyst species *Apteodinium*? *vescum* (late Burdigalian to early Serravallian or N8-N11 in Japan (*175*)), *Cleistosphaeridium ancyreum* (early Eocene to mid Miocene (*176*)), *Cleistosphaeridium placacanthum* (mid Eocene (*176*) to early Tortonian, (10.6 Ma according to the magnetostratigraphy calibration of(*177*), *Quadrina* "incerta" (=Dinocyst XI (late Burdigalian (*126*))) and the acritarch *Quadrina*? *condita* (late Burdigalian-NN4- (*178*) - late Tortonian -NN11- (*179, 180*)). The stratigraphic ranges infer deposition sometime between the late Burdigalian (NN4) and the early Serravallian (18 to 10.4 Ma).

The deposition of the upper segment in 105-AM (meters 140.9 to 34.6) took place sometime between the late Burdigalian and the early late Miocene based on the stratigraphic ranges of *Quadrina*? *condita*, and the rare dinocyst *Trinovantedinium*? *xylochoporum* (late Oligocene - Tortonian (*179*)) and the acritarch *Cyclopsiella elliptica/granosa* complex (late Oligocene – early late Miocene (*181*)). However, *C. ancyreum* and *C. placanthum*, together with other gonyaulacacean dinoflagellate cysts, are absent in the upper sequence in 105-AM. Two possibilities can be considered. Firstly, the upper sequence is younger than mid Miocene, and thus cannot hold *C. ancyreum* or *C. placanthum*. A second possibility assumes that the environment was unfavorable for many dinoflagellate cysts (cf. the low diversity, low richness, high reworking, tidal lithofacies). If the second assumption is followed then a late Burdigalian–Serravallian age can be inferred. Pliocene dinocyst species are absent in the upper marine interval, as are late Miocene marker species.

The stratigraphic interpretation of the marine intervals in the Saltarin (table S1) relies on *Q.*? *condita*, *Trinovantedinium papula* (NN5, Langhian–Tortonian (*179, 180*)) and *T.*? *xylochoporum*. The presence of *Quadrina*? *condita* in the lowest marine interval points to deposition some time during the late Burdigalian to Tortonian. *Trinovantedinium papula* is only found in the upper interval, suggesting an age interval between Langhian and Tortonian.

5.5 Stable carbon-isotope values of bulk organic matter

Stable carbon-isotopes support the age determinations produced by the graphic correlation analysis. $\delta^{13}C$ values are given in table S11. Carbon isotope ratios ($\delta^{13}C$) of Saltarin shows that there is a positive isotopic shift from meters 637 to 535 (table S11, fig. S16). Ratios increase from -28.21 to -25.17 ‰ respectively. This shift seems to correspond to the 18 to 16 Ma global positive $\delta^{13}C$ shift (*182*) (fig. S16), and supports the age of Saltarin produced by graphic correlation for that segment (meter 535 = 15.8 Ma, meter 637 = 17.9 Ma, table S4). Isotopic ratios from meter 535 to the uppermost segment

of the core does not show a clear pattern but a high variance in isotopic values. Its correlation with the global $\delta^{13}C$ record cannot be assessed.

Carbon isotope data ($\delta^{13}C$) of 105-AM does not show a distinct pattern (table S11, fig. S17). Values have high variance making its correlation with the global $\delta^{13}C$ record difficult to assess.

5.6 Molluscan biostratigraphy 105-AM

Mollusks in 105-AM were found in four different samples and can be divided into two assemblages: 52.9 to 53 m, and 79.9 to 83m. Twenty-one species in 11 genera were identified (table S12) and photographed (fig. S18). The molluscan biostratigraphic zones follow (*13, 71*). The 52.9–53 m assemblage could be assigned to either MZ12 zone (the youngest published Pebas fauna so far) but has even more in common with a younger fauna to be published still. Age would be latest middle Miocene or earliest late Miocene. The 79.9–83m assemblage contains an admixture of several faunas. *Charadreon intermedius* is known from MZ7-MZ8, but most of the fauna is typical of MZ9-11 (e.g. *Aylacostoma browni*, *Charadreon glabrum*, *Pachydon trigonalis*). Therefore, the assemblage is assigned to zones MZ9–MZ11 (late middle Miocene). The age of both assemblages supports the age derived from graphic correlation (fig. S19).

section S6. Sites from the literature used in this study

Nine sites that had presented evidence of dinoflagellates and microforaminifera were used in this study. Boonstra et al (*36*) and Hoorn (*21*) studied 49 palynological samples of core 1AS-4AM, one of the few cores studied for palynology in the entire western Amazonia. Sampling density was relatively low (~7.2 meters per sample). These studies found two distinct marine incursions in the early and middle Miocene similar to those reported here. Both marine intervals were added to the paleogeographic maps. Boonstra et al (*36*) and Hoorn (*22*) studied the palynology of three outcrops in Colombian Amazonia, close to 105-AM (Mocagua, Los Chorros 1E and Los Chorros 1W), that contained marine intervals and belong to palynological zone T-15 (*36*). They correspond to the same age interval as the middle Miocene flooding reported here. A third set of studies (*17, 36*) focused on the palynology of three outcrops (Mariñame II, Mariñame III, and Tres Islas III) in northern Amazonas Basin (Caquetá region) that contained marine intervals and were dated as belonging to palynological zone T-13 (*19, 36*). A detailed study of Mariñame III (*19*) found a distinct marine interval at meters 46.7-49.5, zone III, that was is interpreted as an estuarine environment with a large input of terrestrial material. Abundance of marine palynomorphs in zone III is significantly higher than in the zones below and above. This result is in agreement with our interpretation of a marine interval in zone T13. This marine interval is deeper, more saline and of larger time span toward the north (Saltarin site), while is shallower, less saline and shorter in time span toward the south (Mariname and 105 AM sites). Boonstra et al. (*36*) presents three additional outcrops also from the northern Amazonas Basin: Buenos Aires and El Salado, both dated as palynological zone T-15, and Apaporis IV, dated as palynological zone T-14. Thus the middle Miocene in the northern Amazonas Basin appears to span both the top of the palynological zone T-14 and the base of palynological zone T-15. The northern Amazonas Basin region is halfway between Saltarin and 105-AM and it would be

expected to have a longer flooding interval than 105-AM and shorter than Saltarin if flooding progressed southward in both the early Miocene and middle Miocene flooding events. These results were added to the paleogeographic reconstruction in GPlates.

section S7. Other published sites beyond the boundaries of this study

Here we have listed many previously studied sites already studied that we omitted from our analysis either because palynological studies were lacking, thus preventing correlation of our cores to each particular outcrop, or because they were located outside the Amazonas/Solimões and Llanos basins.

-(*18*) analyzed the sedimentology of 16 sites around Iquitos. Each site is represented by an outcrop 15-20 thick exposed along a river bank. All of the sites presented have a diverse degree of marine influence in their sedimentological characteristics, which led the authors to conclude that several tens of high-frequency marine ingressions reached western Amazonia during the Miocene. The ingressions were shallow and restricted. The study indicates palynological zones for each site, but it did not present a list of the palynological contents, thus making correlation with our sites impossible.

-(*72*) analyzed the sedimentology of two outcrops along a river bank near Iquitos and found evidence that sediment accumulation occurred in bay-margin environments that prograded into a shallow, quiescent bay. However, there are no published palynological data that could be used to correlate this study with our sites.

-(*66*) studied eight river and road outcrops in Acre state, about 600 km south of our study sites that belong to the upper part of the Solimões Formation. No palynological study was done, and strata were dated as late Miocene based upon several tuff layers that imply an age of 9 to 3 Ma. The deposits were interpreted as tidally and seasonally influenced estuarine or delta-related and continental strata.

-(*25*) studied five sites in western Brazil, ~500 km south of 105-AM. They are outcrops from the Solimões Formation that are dated as late Miocene (9 to 6.5 Ma), thus being younger than the top of the 105-AM core. Sedimentological analysis indicates that they are avulsive fluvial belts in a floodbasin–floodplain environment with widespread lacustrine swampy deposits, stacked channel deposits, and paleosols. No evidence of marine deposition was found. There are additional palynological data from the core 1-AS-32-AM, which was drilled about 160k west of core 105-AM. However, neither the stratigraphic position nor palynomorph content of each sample was provided.

-(*65*) analyzed the palynological content of two cores, 1-AS-19-AM and 1-AS-27-AM, that are 80 km and 160 km east of core 105-AM respectively. However, the sample density that was used (one sample/~27 meters in 19-AM and one sample/~12 meters in 27-AM) was much lower than ours (~one sample every 3 stratigraphic meters). This low sampling density could miss a possible marine incursion, given that 105-AM the two marine intervals were 9.3 and 4.5 meters thick. Therefore, we prefer to omit both cores until a higher resolution study of both of them is completed.

-(*10*) analyzed the sites already reported by (*25*) and (*65*) and reached a similar conclusion as reported in 1997, i.e., that there is no evidence of marine incursions during the late Miocene.

-(*20*) analyzed multiple outcrops in the Acre basin, about 600 km south of 105-AM. They report tidal deposits dated as 10 to 8 Ma; however, they did not provide either the fossils used to date these sites or the stratigraphic position of the studied outcrops.
-(*70*) studied seven outcrops of the upper Pebas Formation, each 5-8 meters thick, along a ~40 km river profile, about 420 km southwest of 105-AM. Some levels contain sediments interpreted to represent a marine incursion. One of the sites (# 6) was dated as late Miocene based upon the analysis of the palynological content of one sample.

-(*69*) studied five sections of the Nauta Formation, 8 to 12 m thick each, along a 26 km road, about 350 km southwest of 105-AM. The sections were dated as late Miocene based on a single pollen sample taken in outcrop #5. Results indicate accumulation in a shallow, marginal-marine channel complex dominated by tidal channels developed in a delta plain.

-(*28*) studied five sections of the Beni-Mamore basin in Bolivia, 2 to 15 meters each, spread along a 200 km profile. Sites were dated as late Miocene based upon lithostratigraphic correlation with the Cobija Formation. Results indicate the transition from a tide-influenced depositional system to a fully continental depositional system.

-(*13*) studied ditch cuttings of three wells drilled in Loreto (Peru), about 700 km west of 105-AM. Lithofacies and electric logs were studied. Mollusks were used for chronological control. No palynological data were reported. The Pebas Formation is dominated by lacustrine and swamp settings, a mosaic of lakes, swamps, and fluvial belts with some tidal influence. Pebas accumulation ends between 8 and 10 Ma, and the lake system ends.

-(*86*) studied a 18-m-thick section of the Pebas Formation in Loreto Peru, about 250 km east of 105-AM. The section was dated as middle Miocene, but palynological data were not reported. No marine evidence was found other than the presence in two samples of juvenile shells of *Corbula cotuhensis,* an indicator of brackish conditions. The system consisted of mostly freshwater swamp to lacustrine conditions in a long-lived lake/wetland system at sea level and open to marginal marine settings.

-(*79*) studied ten outcrops, 5–15 meters each, of the upper Solimões Formation in southwest Amazonas state, about 300 km south of 105-AM. Strata were dated as late Miocene based on three pollen taxa (*Cyathidites annulatus, Echitricolporites maristellae*, and *Grimsdalea magnaclavata*). Sedimentological analysis indicates fluvial deposits of an anastomosing river; no evidence of marine incursions was found. Further research using Ostracoda confirmed the lack of marine influence in this region (*80*).

-(*90*) studied the ostracod *Cyprides* content and taxonomy of 44 samples taken from the 400-m-thick core 1AS-10-AM, ~80 km south of 105-AM (~one sample each 9 m).

Numerous new species were proposed. The upper 220 meters of the core is dated as late middle Miocene to early late Miocene using the ostracod zonation of Torres 2006 (*88*).

-(*23*) studied the palynological content of three outcrops, 1.7 to 10 meters each, in Colombian Amazonia. None of them found strong evidence of marine palynomorphs.

-(*36*) studied the palynological content of several previously studied outcrops (*17, 21-23*) that we had considered for this study as they contained marine intervals (see above). They reported a new site, Nuevo Horizonte in the Peruvian Amazon, ~350 km west of 105-AM in the Marañon/Acre Basin. Nuevo Horizonte has a well-defined marine interval, but the authors provided neither the section nor the complete palynological data.

-(*29*) studied the strontium, oxygen, and carbon isotope composition of mollusk shells in several outcrops. Several samples, from two Buenos Aires sites near the Chorros sites, showed evidence of marine incursion that was dated as middle Miocene by (*36*). However, neither of these two studies presented the full palynological dataset. All other data analyzed indicated fresh water. Twenty samples from core 1AS-4a-were analyzed, but sample density was too low to be conclusive (one sample each 22 meters).

-(*183*) studied the stratigraphy and environments of the Contamana region in central Peruvian Amazonia. They reported the occurrence of *Crassostrea* Oyster beds.

fig. S1. Map of northwestern South America showing the sedimentary basins discussed in the text and the structural features that divide them. Locations of basins and arches after (*21, 34, 107-110*). Elevation after ETOPO1 (*184*).

fig. S2. Location of the nine wells in the Llanos Basin, two wells in the Amazonas/Solimões Basin, and 13 seismic lines used for this study (geographic coordinates in tables S5 and S6). Main figure: location of the nine wells in the Llanos, two wells in the Amazonas/Solimões Basin, and 13 seismic lines used for this study (geographic coordinates in tables S5 and S6). Selected outcrop localities have report of marine influence during the Miocene (*17, 21*) for coordinates and information refer to table S1. Base map from GTOPO30 (*185*).

fig. S3. Sedimentological and sequence stratigraphic interpretation of the Saltarin well (see details of interpretation in table S7). Supplementary Online File 5 (At Dryad Digital Repository, doi:10.5061/dryad.53m76) contains the tables needed to reproduce the stratigraphic column and an extended version of this column including comments.

fig. S4. Graphic correlation of Saltarin versus 105-AM using geological time as scale in both axes, rather than stratigraphic thickness. Correlation was obtained by the sedimentological and palynological record of both cores. It shows the time distribution of the three broad depositional systems (Continental, Marginal and Marine). The middle Miocene interval (MMI) has a longer duration than the early Miocene interval (EMI).

fig. S5. Photomicrographs of selected dinoflagellate cysts and acritarchs. Scale bar is 10 μm. E.F.: England Finder coordinates. (A). *Apteodinium? vescum* Matsuoka. Core 1-AS-105-AM, sample 22454, E.F.: H44/1, high focus on wall and archeopyle outline. (B). *Cleistosphaeridium ancyreum* (Cookson and Eisenack) Eaton et al. Core 1-AS-105-AM, sample 22460, E.F.: U47, high focus on processes. (C). *Cleistosphaeridium placacanthum* (Deflandre and Cookson) Eaton et al. Core 1-AS-105-AM, sample 22454, E.F.: X23, high focus on wall and processes. (D). *Quadrina* "incerta" (=Dinocyst XI of Lenoir and Hart, 1986). Core 1-AS-105-AM, sample 22454, E.F.: E41/1. High focus on wall and protrusions. (E). *Lingulodinium machaerophorum* (Deflandre and Cookson) Wall. Core 1-AS-105-AM, sample 22294, E.F.: K46, high focus on archeopyle margin, wall and processes. (F). *Operculodinium israelianum* (Rossignol) Wall. Core 1-AS-105-AM, sample 22451, E.F.: Y9/2, optical section. (G). *Polysphaeridium subtile* Davey and Williams. Core Saltarin-1A, sample 510.03, E.F.: V37/2, optical section. (H). *Trinovantedinium papula* de Verteuil and Norris. Core Saltarin-1A, sample 468.84, E.F.: E14/2, high focus on wall and processes. (I). *Trinovantedinium? xylochoporum* de Verteuil and Norris. Core Saltarin-1A, sample 409.52, E.F.: L41, high focus on wall and processes. (J). *Tuberculodinium vancampoae* (Rossignol) Wall. Core Saltarin-1A, sample 409.52, E.F.: D9/4, optical section. (K). *Cyclopsiella elliptica/granosa* complex sensu de Verteuil and Norris. Core 1-AS-105-AM, sample 22158, E.F.: N23/1, optical section. (L). *Quadrina? condita* de Verteuil and Norris. Core Saltarin-1A, sample 409.52, E.F.: F46, optical section.

fig. S6. Carcharhiniformes gen. et sp. indet. tooth from the core Saltarin, Carbonera C2 Formation, early Miocene, 630.08 m, specimen MUN STRI-40967.
(A) lingual view. (B), labial view.

fig. S7. Dactyl of raptorial appendage (second thoracopod) of a fossil mantis shrimp from the Carbonera Formation, early Miocene, Colombia, MUN STRI-40281. (A) Core where the specimen was found. (B) Composite Scanning Electron Microscope image of the raptorial appendage. (C) Close-up of the first and most distal spine of the raptorial appendage, showing details of the barbed bands. (D) Close-up of the last and more posterior spines 5–7 of the raptorial appendage, showing details of the barbed bands and a narrow carina on their dorsal margin.

fig. S8. Sedimentological and sequence stratigraphic interpretation of the 105-AM well (see details of interpretation in table S8). Supplementary Online File 5 (At Dryad Digital Repository, doi:10.5061/dryad.53m76) contains the tables needed to reproduce the stratigraphic column and an extended version of this column including comments.

fig. S9. Stratigraphic correlation of the two major marine incursions (EMI and MMI) from the Saltarin well to the northernmost expression of the Vaupés Arch in the subsurface (well I). This correlation uses Gamma ray (GR) and spontaneous potential (SP) electric logs, lithology (L) and reported presence of marine to brackish water fossils in well cuttings (*53*).

fig. S10. Stratigraphic correlation of the two major marine incursions (EMI and MMI) along the northern Amazonas/Solimões Basin. Age control is based mainly from the palynological analysis of well 105-AM. This correlation shows how the EMI spans both the top of the palynological biozone T-12 and the base of T-13 and the MMI spans both the top of biozone T-14 and the base of T-15. The thickness of both incursions decreases outward (from zone 1 to zone 7), as well as eastward. Location of source areas (Guiana Shield) is to the northeast. Zones after Jaramillo et al. (*56*)

fig. S11. Graphic correlation between the standard composite section of Jaramillo *et al.* (*56*) and core Saltarin. Notice the border effect that artificially increases the LAD (Last Appearance Datum) near the top of Saltarin and increases the FAD (First Appearance Datum) near the base of the section. Palynological Zones after Jaramillo et al. (*56*). Miocene time table after Hilgen et al. (*64*). The segment points of the LOC (Line of Correlation) are in table S9, and all the events of the correlation in this figure are in Supplementary Online File 4.1. (At Dryad Digital Repository, doi:10.5061/dryad.53m76)

fig. S12. Graphic correlation between the standard composite section of Jaramillo *et al.* (*56*) and core 105-AM. Notice the border effect that artificially increases the LAD (Last Appearance Datum) near the top of 105 and increases the FAD (First Appearance Datum) near the base of the section. Palynological Zones after Jaramillo et al. (*56*), Miocene time table after Hilgen et al. (*64*). The segment points of the LOC (Line of Correlation) are in table S9, and all the events of the correlation in this figure are in Supplementary Online File 4.2. (At Dryad Digital Repository, doi:10.5061/dryad.53m76)

fig. S13. Seismic profiles in the Llanos Basin (see location in fig. S2; interpretation only at one extreme of the line) illustrate the seismic facies of the two marine incursions (EMI and MMI). Seismic line 1 shows the seismic facies with absence of seismic reflectors of the two major marine incursions and the location of the Saltarin well. Seismic lines 7 and 5 illustrate the lateral change of seismic facies of the Leon Formation, as more seismic reflectors are evident above the Vaupés Arch, suggesting a lateral change from homogeneous lithology of marine environments, to a interbeds of sandstones and mudstones more characteristic of Marginal environments. Notice how the seismic reflectors of the middle Miocene Leon Formation are deformed by late Miocene deformation.

fig. S14. Interpreted 2D seismic profiles showing the contrasting difference of seismic facies between undifferentiated Cenozoic and Cretaceous units in the Amazonas/Solimões Basin (see fig. S2 for the location of seismic lines). Cenozoic seismic reflectors are discontinuous and not parallel among them, and the amplitude of the peaks and troughs varies laterally.

fig. S15. Graphic correlation between the cores Saltarin and 105-AM. Notice the border effect that artificially increases the LAD (Last Appearance Datum) near the top of 105 and increases the FAD (First Appearance Datum) near the base of the section. Line of Correlation is derived from the correlation of both sections among each other, and each individual section versus the Composite (figs. S11 and S12). The segment points of the LOC (Line of Correlation) are in table S9, and all the events of the correlation in this figure are in Supplementary Online File 4.3. (At Dryad Digital Repository, doi:10.5061/dryad.53m76).

fig. S16. Carbon isotope data ($\delta^{13}C$) versus stratigraphic position in core Saltarin on the left panel. Raw data and a five-sample running average (red line) shows that there is a positive isotopic shift from meters 637 to 535 (table S6). This shift seems to correspond to the 18 to 16 Ma global positive $\delta^{13}C$ shift, right panel (*182*).

fig. S17. Carbon isotope data ($\delta^{13}C$) versus stratigraphic position in core 105-AM. Raw data and a 5-sample running average (red line) do not show a distinct pattern that could be correlated to the global $\delta^{13}C$ record. Sample at meter 262.3 yielded a high value (-19.64 ‰) and therefore it is not plotted in the graphic as it is beyond the X-axis range (-28.5 to -24 ‰).

fig. S18. Photographs of shells from core 105-AM. (A) to (G) are bivalves for which exterior and interior views are shown (1's and 2's, respectively). (H) to (P) are gastropods for which rear and front views are shown (1's and 2's, respectively). (A) *Corbula cotuhensis* Wesselingh & Anderson, 53 m (B) *Mytilopsis sallei* Récluz, 53 m (C) *Pachydon carinatus* Conrad, 83 m (D) *Pachydon cuneatus* Conrad, 52.9 m (E) *Pachydon ledaeformis* Dall, 53 m (F) *Pachydon telliniformis* Wesselingh, 53 m. (G) *Pachydon trigonalis* Nuttall, 79.9 m (H) *Aylacostoma browni* Etheridge, 53 m (I) *Charadreon glabrum* Wesselingh, 79.9 m (J) *Charadreon intermedius* Wesselingh, 79.9 m (K) *Dyris*

bicarinatus bicarinatus Wesselingh, 53 m (L) *Dyris ortoni* Gabb, 79.9 m (M) *Feliconcha feliconha* Wesselingh, 79.9 m (N) *Toxosoma grande* Wesselingh, 53 m (O) *Tryonia nuttalli* Wesselingh, 53 m (P) *Tryonia scalarioides scalarioides* Etheridge, 53 m

fig. S19. Molluscan biostratigraphy of core 105-AM. Mollusks at meter 52.9-53 indicate zone MZ12 to MZ13 (latest middle Miocene to earliest late Miocene). Assemblage at meter 79.9-83 m indicates zone MZ9 to MZ11 (molluscan Zones after (*71*)). Molluscan biostratigraphy supports the age derived from Graphic Correlation.

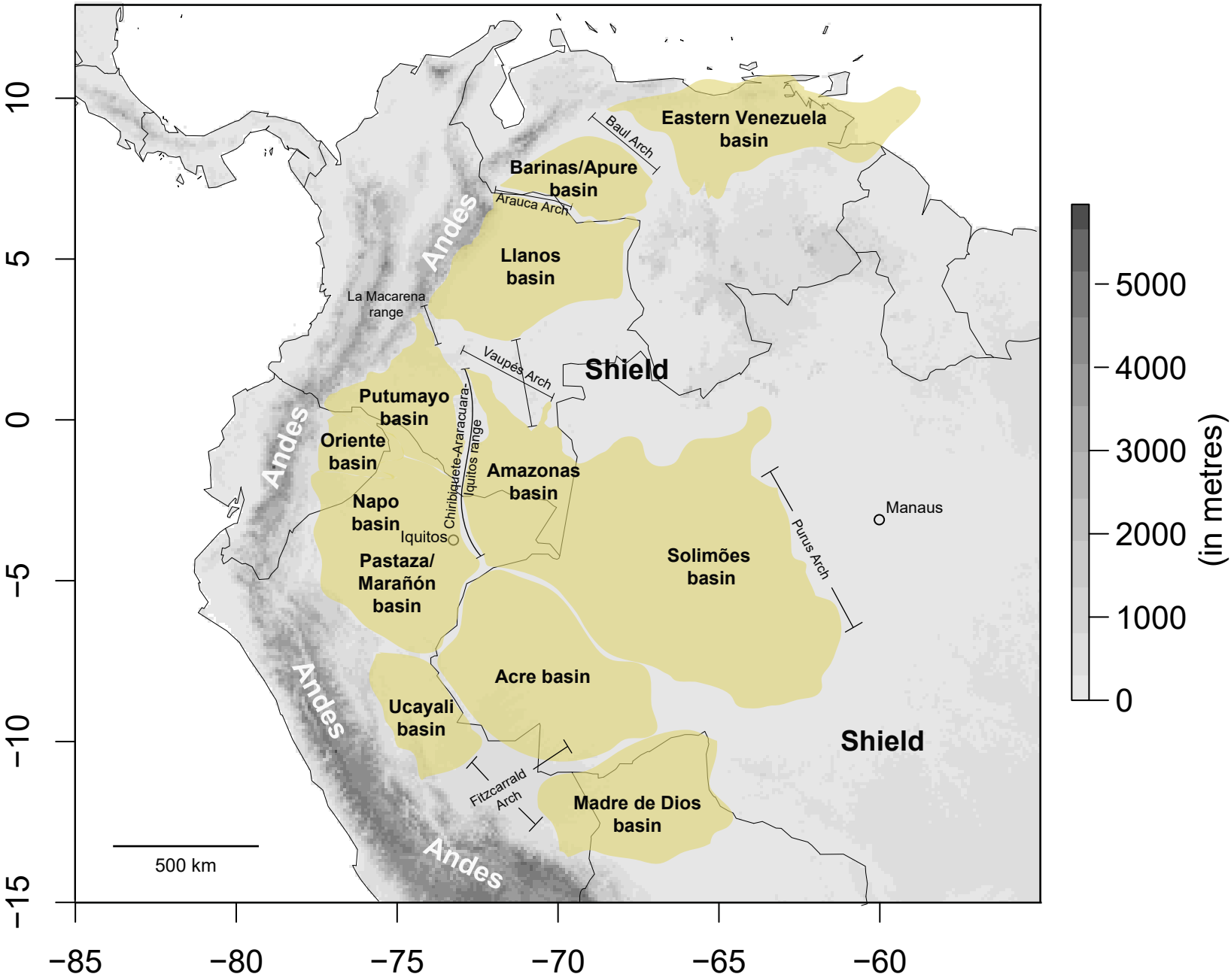

fig. S1. Map of north-western South America showing the sedimentary basins discussed in the text and the structural features that divide them. Locations of basins and arches after (*21, 34, 107-110*). Elevation after ETOPO1 (*184*).

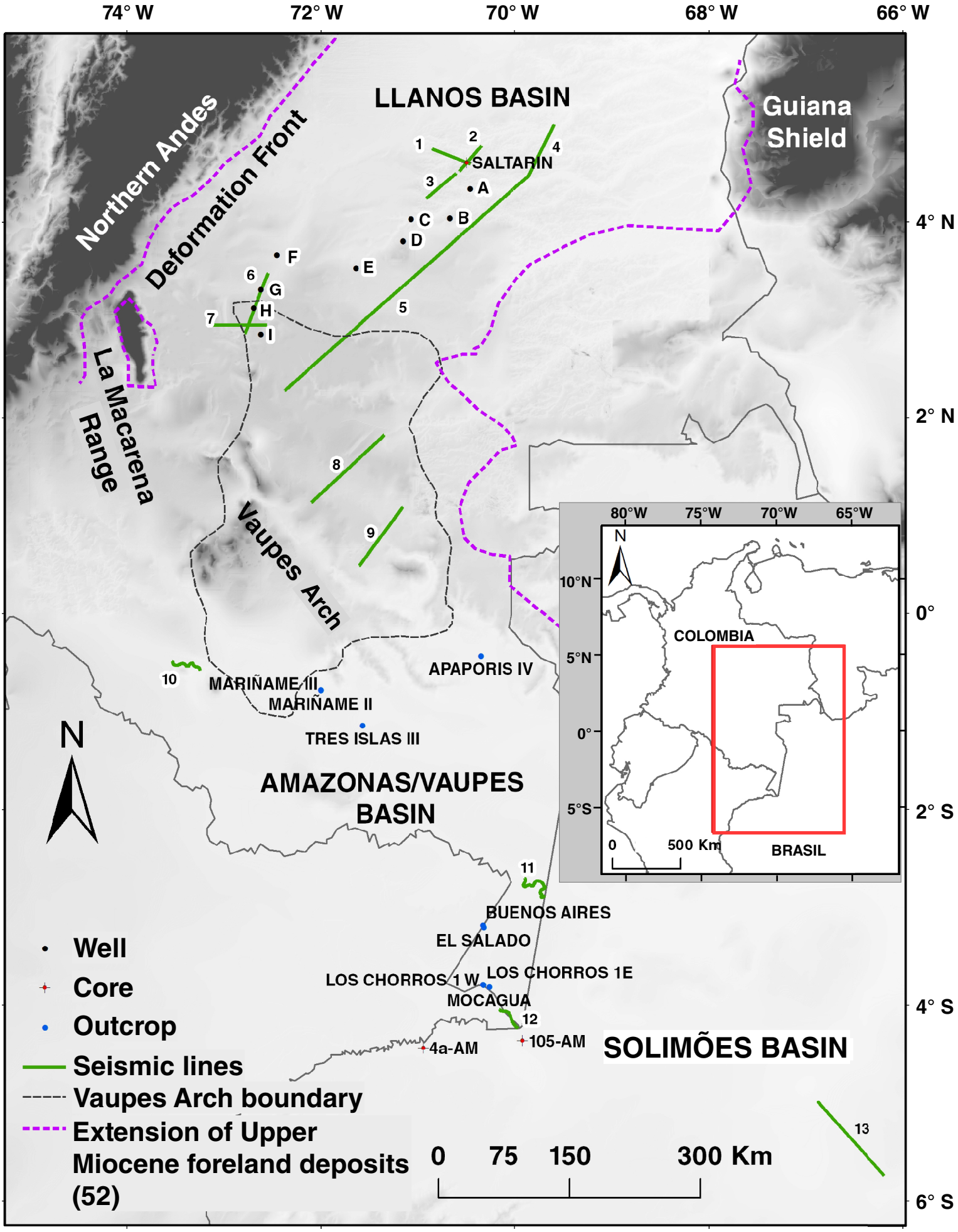

fig. S2. Location of the seismic lines and studied sites. Inset map: Location of the study area covering the Llanos Basin and the northern Amazonas/Solimões Basin.Main figure: location of the nine wells in the Llanos, two wells in the Amazonas/Solimões Basin, and 13 seismic lines used for this study (geographic coordinates in tables S5 and S6). Selected outcrop localities have report of marine influence during the Miocene (17, 21) coordinates and information refer to table S1. Base map from GTOPO30 (185).

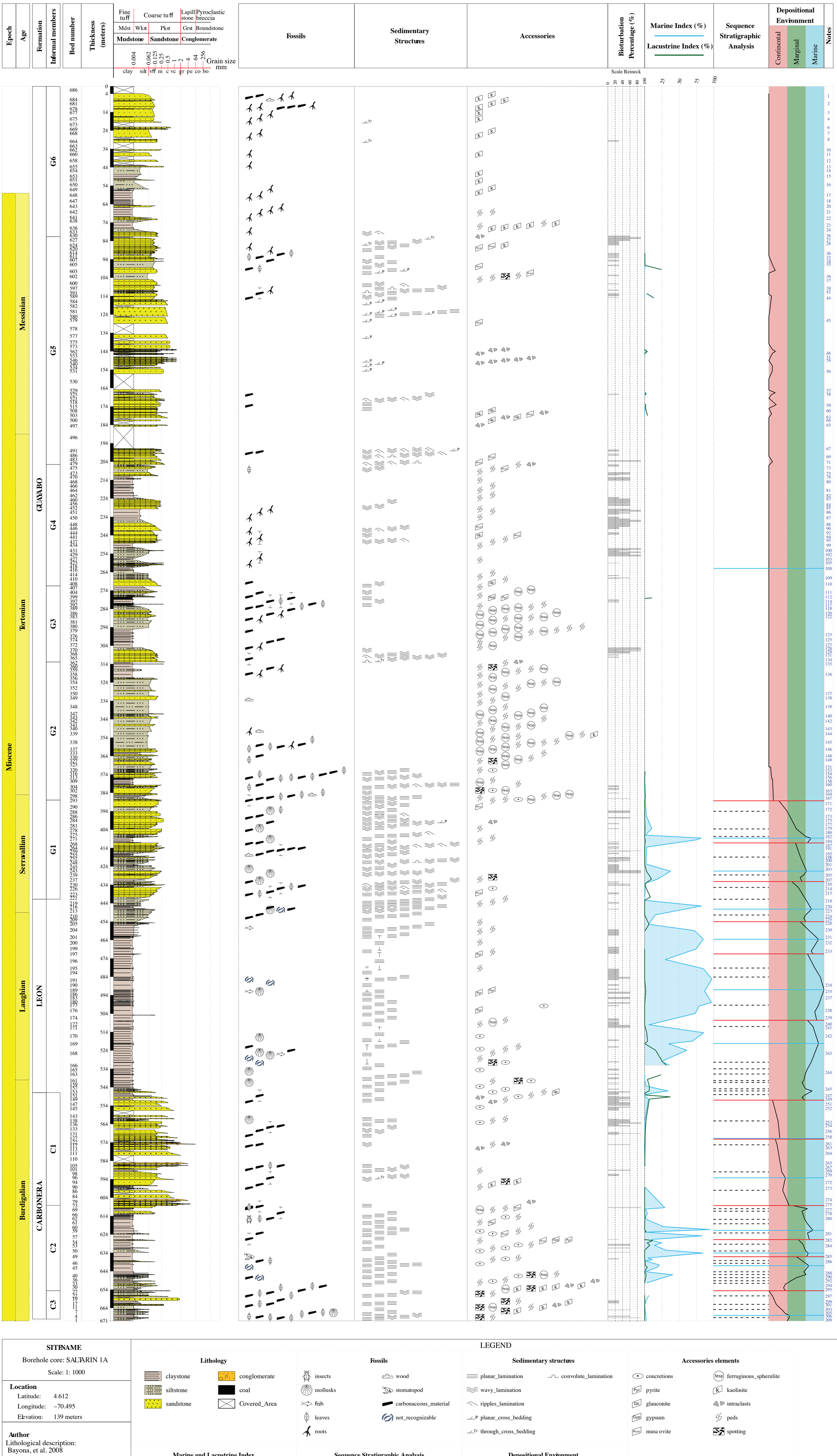

fig. S3. Sedimentological and sequence stratigraphic interpretation of the Saltarin well (see details of interpretation in table S7). Supplementary Online File 5 (At Dryad Digital Repository, doi:10.5061/dryad.53m76) contains the tables needed to reproduce the stratigraphic column and an extended version of this column including comments.

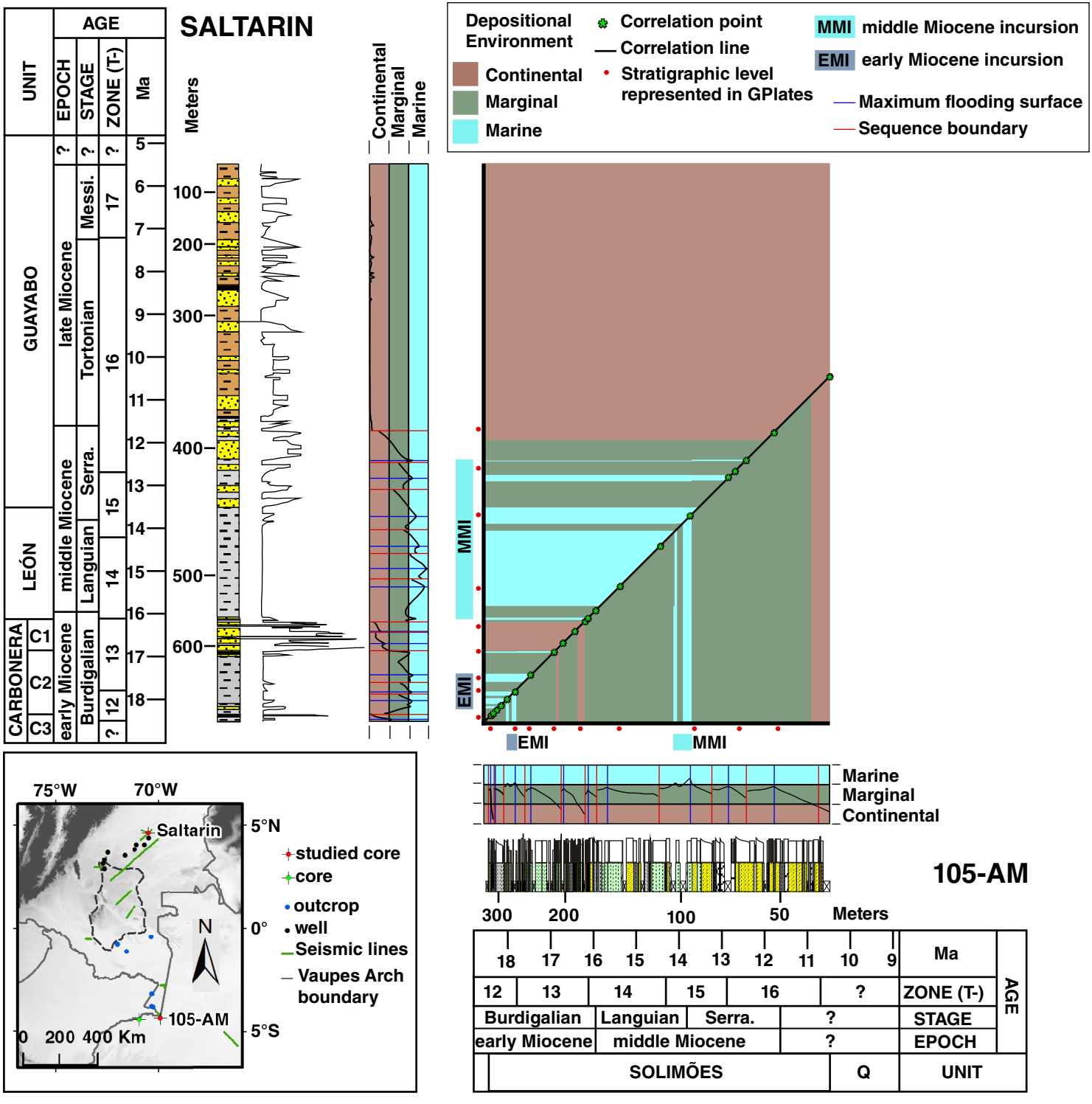

fig. S4. Graphic correlation of Saltarin vs 105-AM using geological time as scale in both axes, rather than stratigraphic thickness. Correlation was obtained by the sedimentological and palynological record of both cores. It shows the time distribution of the three broad depositional systems (Continental, Marginal and Marine). The middle Miocene interval (MMI) has a longer duration than the early Miocene interval (EMI).

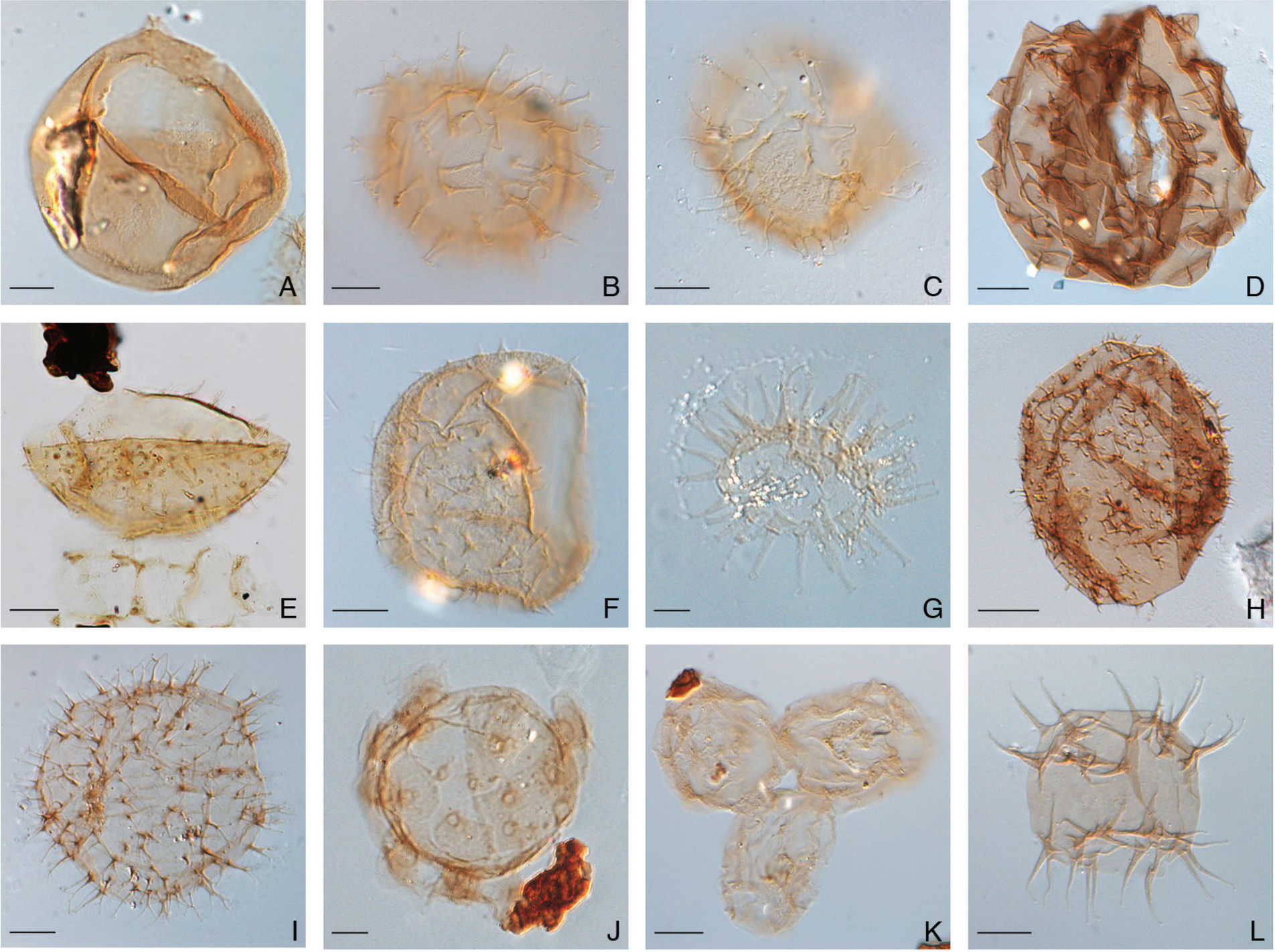

fig. S5. Photomicrographs of selected dinoflagellate cysts and acritarchs. Scale bar is 10 µm. E.F.: England Finder coordinates. (A). *Apteodinium*? *vescum* Matsuoka. Core 1-AS-105-AM, sample 22454, E.F.: H44/1, high focus on wall and archeopyle outline. (B). *Cleistosphaeridium ancyreum* (Cookson and Eisenack) Eaton et al. Core 1-AS-105-AM, sample 22460, E.F.: U47, high focus on processes. (C). *Cleistosphaeridium placacanthum* (Deflandre and Cookson) Eaton et al. Core 1-AS-105-AM, sample 22454, E.F.: X23, high focus on wall and processes. (D). *Quadrina* "incerta" (=Dinocyst XI of Lenoir and Hart, 1986). Core 1-AS-105-AM, sample 22454, E.F.: E41/1. High focus on wall and protrusions. (E). *Lingulodinium machaerophorum* (Deflandre and Cookson) Wall. Core 1-AS-105-AM, sample 22294, E.F.: K46, high focus on archeopyle margin, wall and processes. (F). *Operculodinium israelianum* (Rossignol) Wall. Core 1-AS-105-AM, sample 22451, E.F.: Y9/2, optical section. (G). *Polysphaeridium subtile* Davey and Williams. Core Saltarin-1A, sample 510.03, E.F.: V37/2, optical section. (H). *Trinovantedinium papula* de Verteuil and Norris. Core Saltarin-1A, sample 468.84, E.F.: E14/2, high focus on wall and processes. (I). *Trinovantedinium*? *xylochoporum* de Verteuil and Norris. Core Saltarin-1A, sample 409.52, E.F.: L41, high focus on wall and processes. (J). *Tuberculodinium vancampoae* (Rossignol) Wall. Core Saltarin-1A, sample 409.52, E.F.: D9/4, optical section. (K). *Cyclopsiella elliptica*/*granosa* complex sensu de Verteuil and Norris. Core 1-AS-105-AM, sample 22158, E.F.: N23/1, optical section. (L). *Quadrina*? *condita* de Verteuil and Norris. Core Saltarin-1A, sample 409.52, E.F.: F46, optical section.

fig. S6. Carcharhiniformes gen. et sp. indet. tooth from the Saltarin core, Carbonera C2 Formation, early Miocene, meter 630.08, specimen MUN STRI-40967. (A) lingual view. (B), labial view.

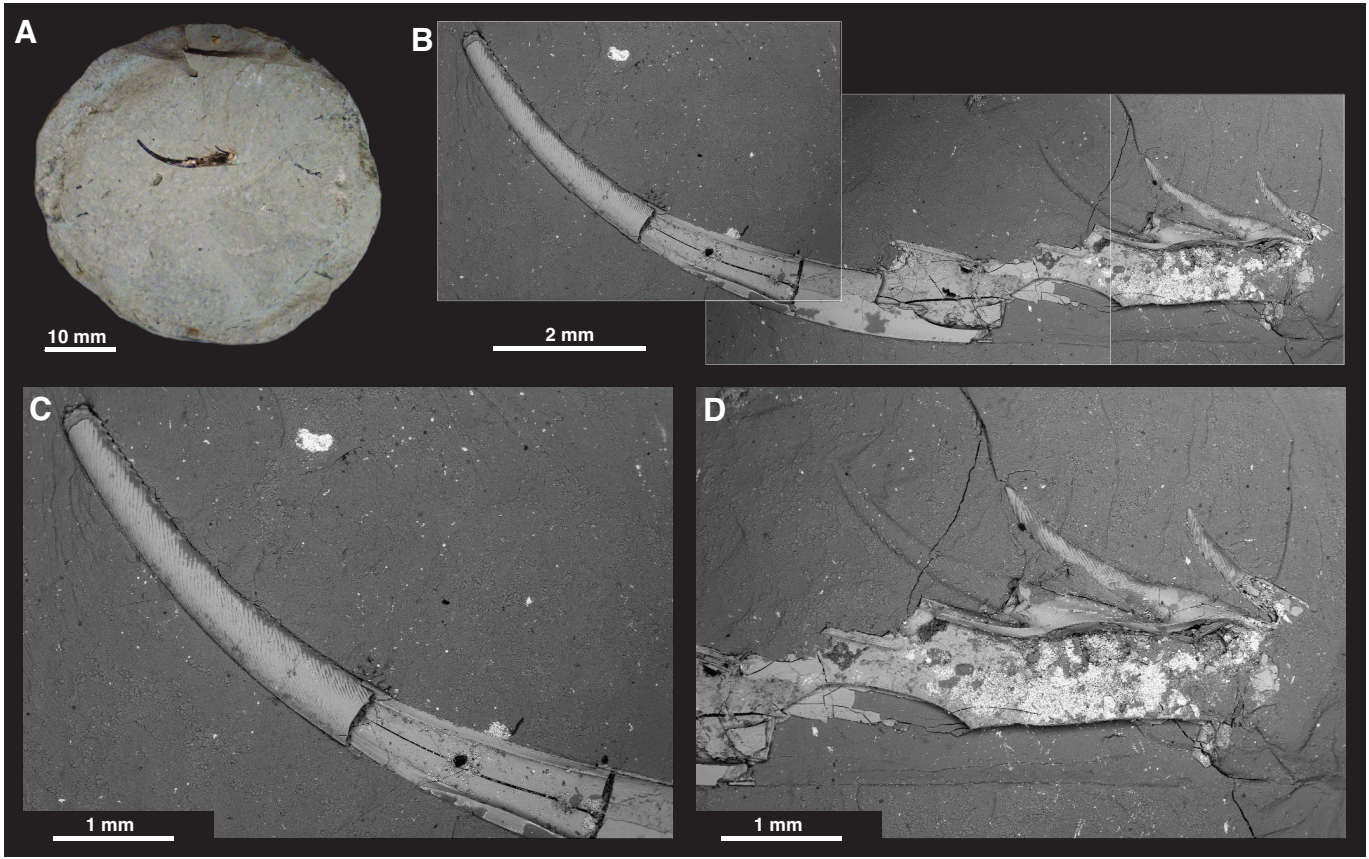

fig. S7. Dactyl of raptorial appendage (second thoracopod) of a fossil mantis shrimp from the Carbonera Formation, early Miocene, Colombia. Specimen MUN STRI-40281. (A) Core where the specimen was found. (B) Composite Scanning Electron Microscope image of the raptorial appendage. (C) Close-up of the first and most distal spine of the raptorial appendage, showing details of the barbed bands. (D) Close-up of the last and more posterior spines 5–7 of the raptorial appendage, showing details of the barbed bands and a narrow carina on their dorsal margin.

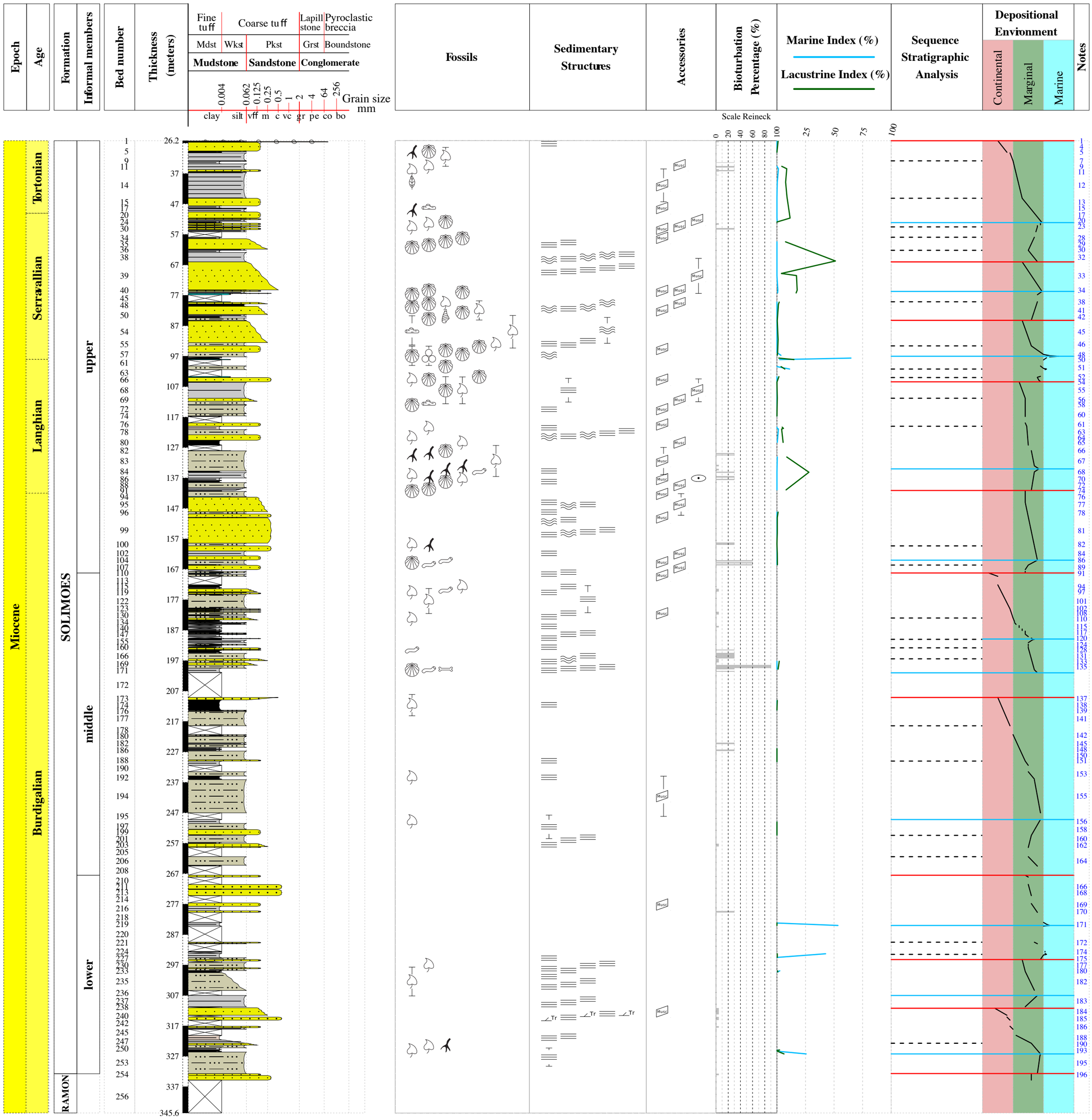

fig. S8. Sedimentological and sequence stratigraphic interpretation of the 105-AM well (see details of interpretation in table S8). Supplementary Online File 5 (At Dryad Digital Repository, doi:10.5061/dryad.53m76) contains the tables needed to reproduce the stratigraphic column and an extended version of this column including comments.

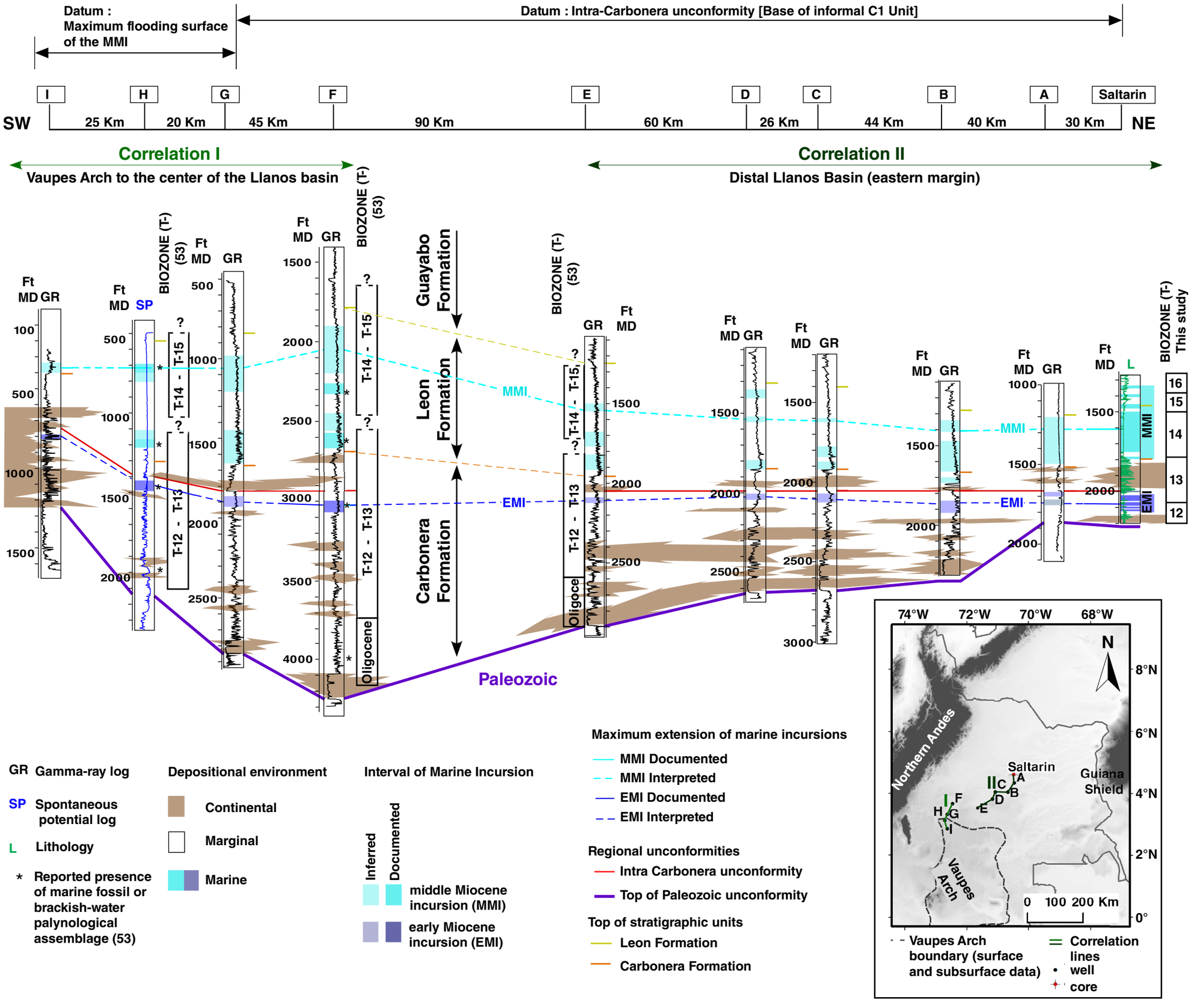

fig. S9. Stratigraphic correlation of the two major marine incursions (EMI and MMI) from the Saltarin well to the northernmost expression of the Vaupés Arch in the subsurface (well I). This correlation uses Gamma ray (GR) and spontaneous potential (SP) electric logs, lithology (L) and reported presence of marine to brackish water fossils in well cuttings (53).

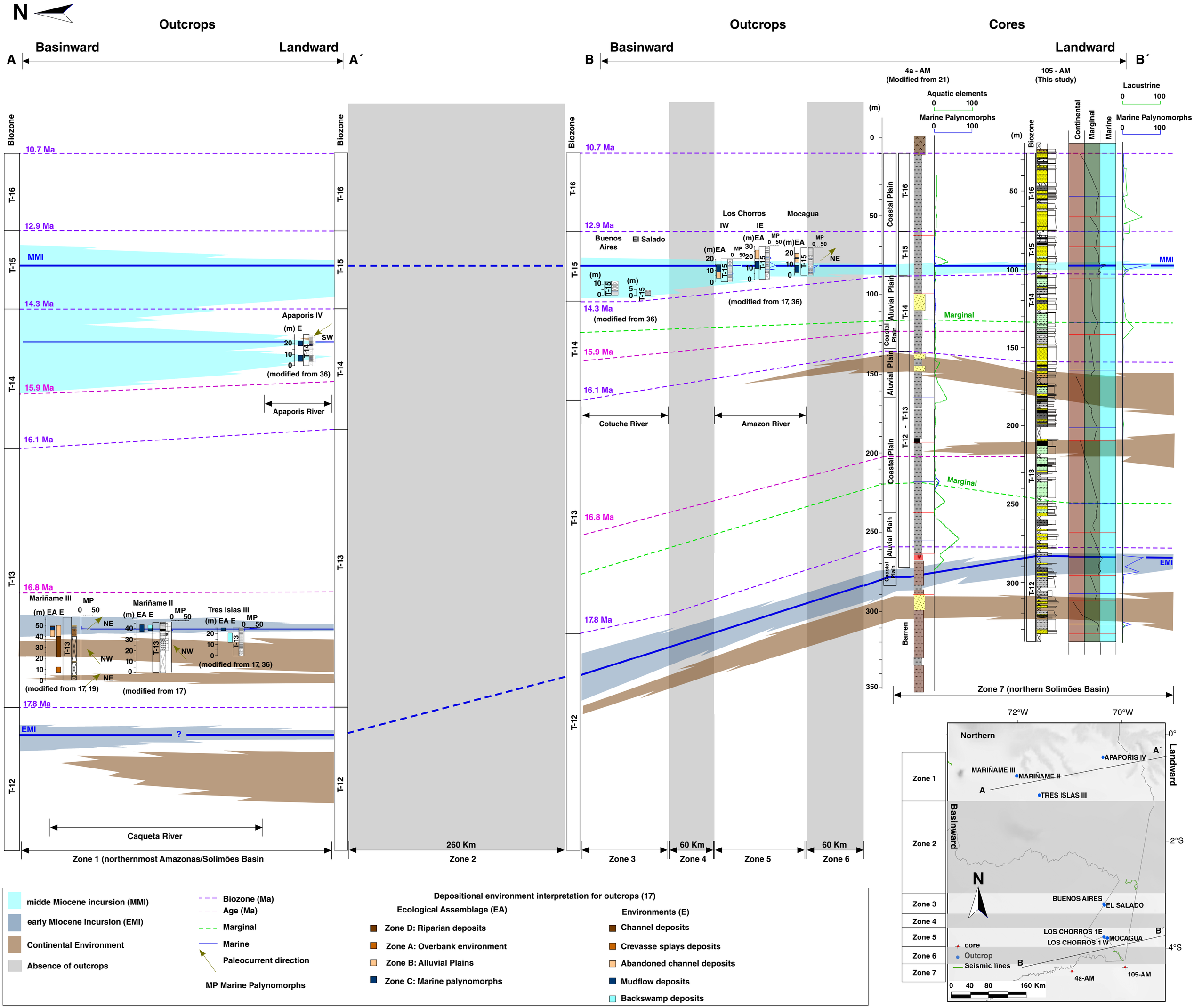

fig. S10. Stratigraphic correlation of the two major marine incursions (EMI and MMI) along the northern Amazonas/Solimões Basin. Age control is based mainly from the palynological analysis of well 105-AM. This correlation shows how the EMI spans both the top of the palynological biozone T-12 and the base of T-13 and the MMI spans both the top of biozone T-14 and the base of T-15. The thickness of both incursions decreases outward (from zone 1 to zone 7), as well as eastward. Location of source areas (Guiana Shield) is to the northeast. Zones after Jaramillo et al. (56)

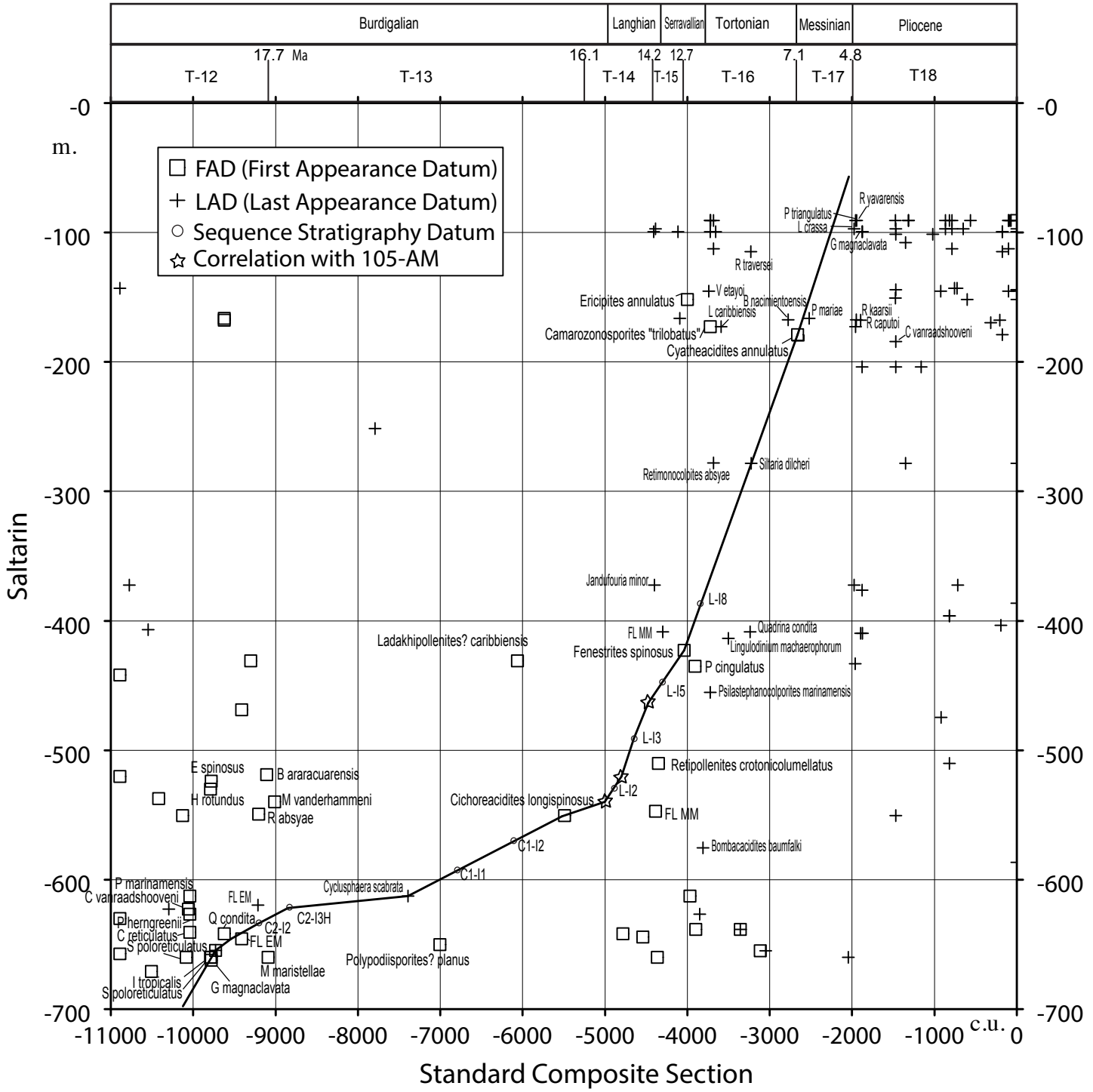

fig. S11. Graphic Correlation between the Standard Composite Section of Jaramillo et al. *(56)* and core Saltarin. Notice the border effect that artificially increases the LAD (Last Appearance Datum) near the top of Saltarin and increases the FAD (First Appearance Datum) near the base of the section. Palynological Zones after Jaramillo et al. *(56)*. Miocene time table after Hilgen et al. *(64)*. The segment points of the LOC (Line of Correlation) are in table S9, and all the events of the correlation in this figure are in Supplementary Online File 4.1. (At Dryad Digital Repository, doi:10.5061/dryad.53m76)

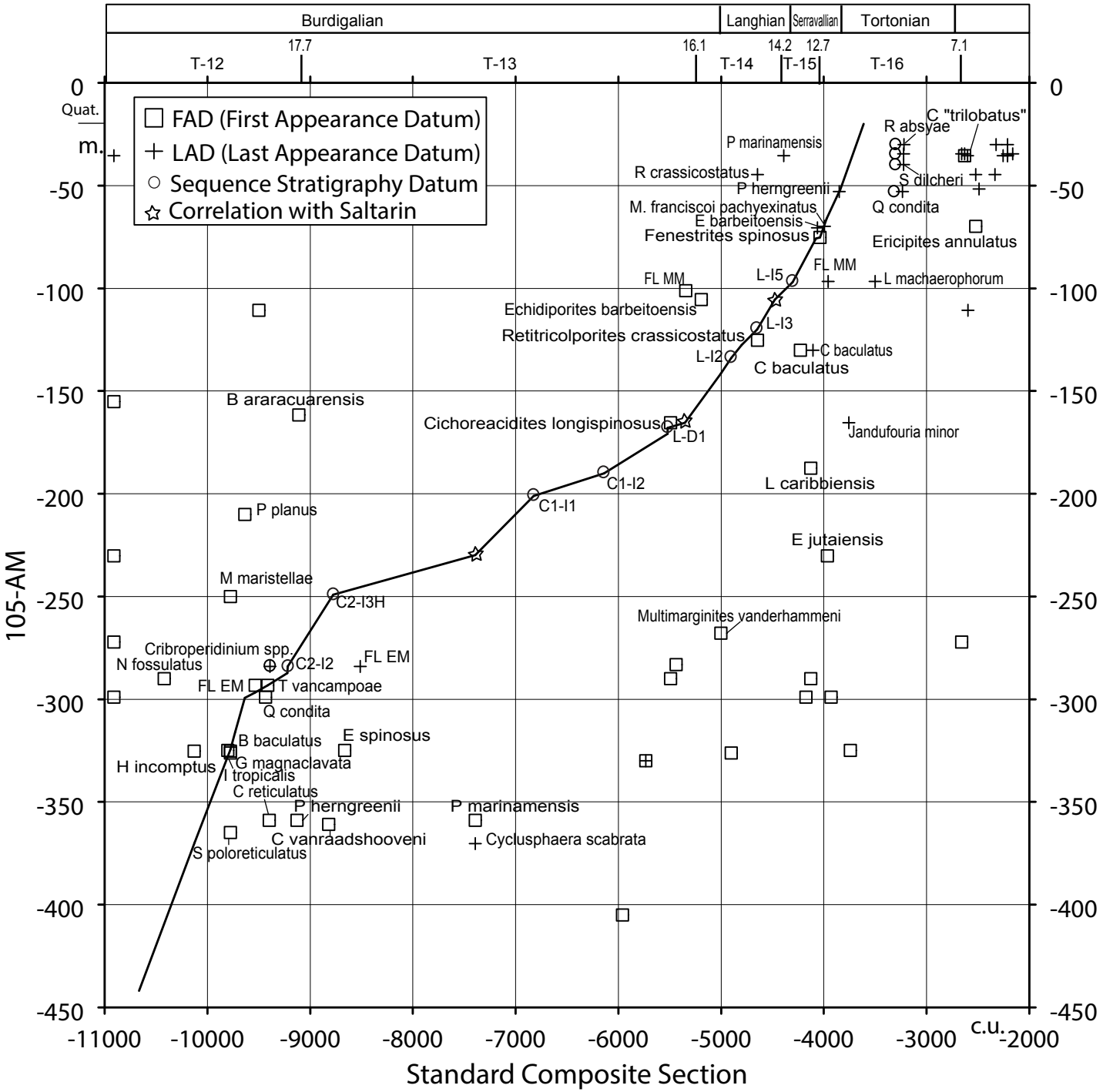

fig. S12. Graphic Correlation between the Standard Composite Section of Jaramillo et al. *(56)* and core 105-AM. Notice the border effect that artificially increases the LAD (Last Appearance Datum) near the top of 105 and increases the FAD (First Appearance Datum) near the base of the section. Palynological Zones after Jaramillo et al. *(56)*, Miocene time table after Hilgen et al. *(64)*. The segment points of the LOC (Line of Correlation) are in table S9, and all the events of the correlation in this figure are in Supplementary Online File 4.2. (At Dryad Digital Repository, doi:10.5061/dryad.53m76)

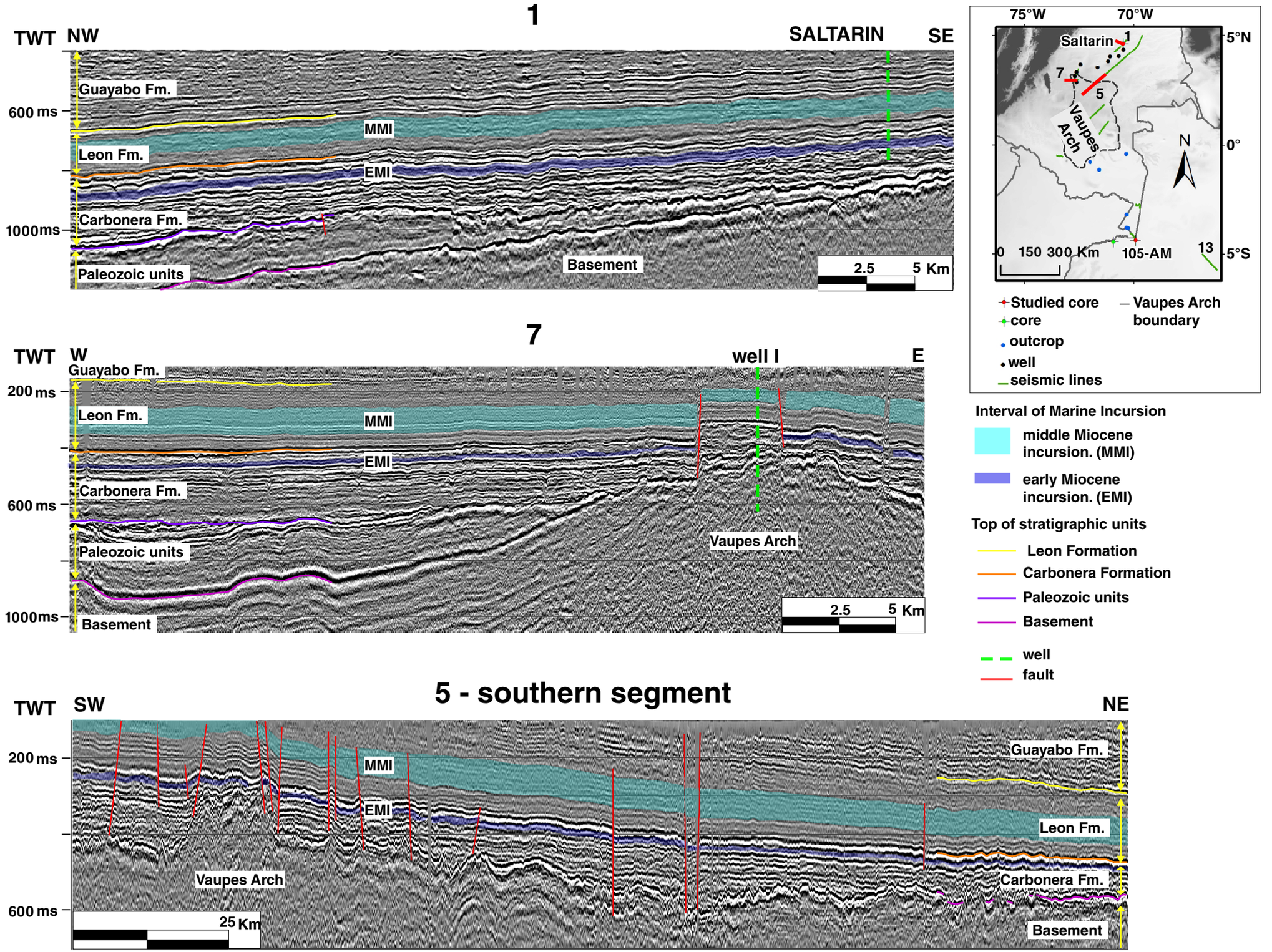

fig. S13. Seismic profiles in the Llanos Basin (see location in fig. S2; interpretation only at one extreme of the line) illustrate the seismic facies of the two marine incursions (EMI and MMI). Seismic line 1 shows the seismic facies with absence of seismic reflectors of the two major marine incursions and the location of the Saltarin well. Seismic lines 7 and 5 illustrate the lateral change of seismic facies of the Leon Formation, as more seismic reflectors are evident above the Vaupés Arch, suggesting a lateral change from homogeneous lithology of marine environments, to a interbeds of sandstones and mudstones more characteristic of Marginal environments. Notice how the seismic reflectors of the middle Miocene Leon Formation are deformed by late Miocene deformation.

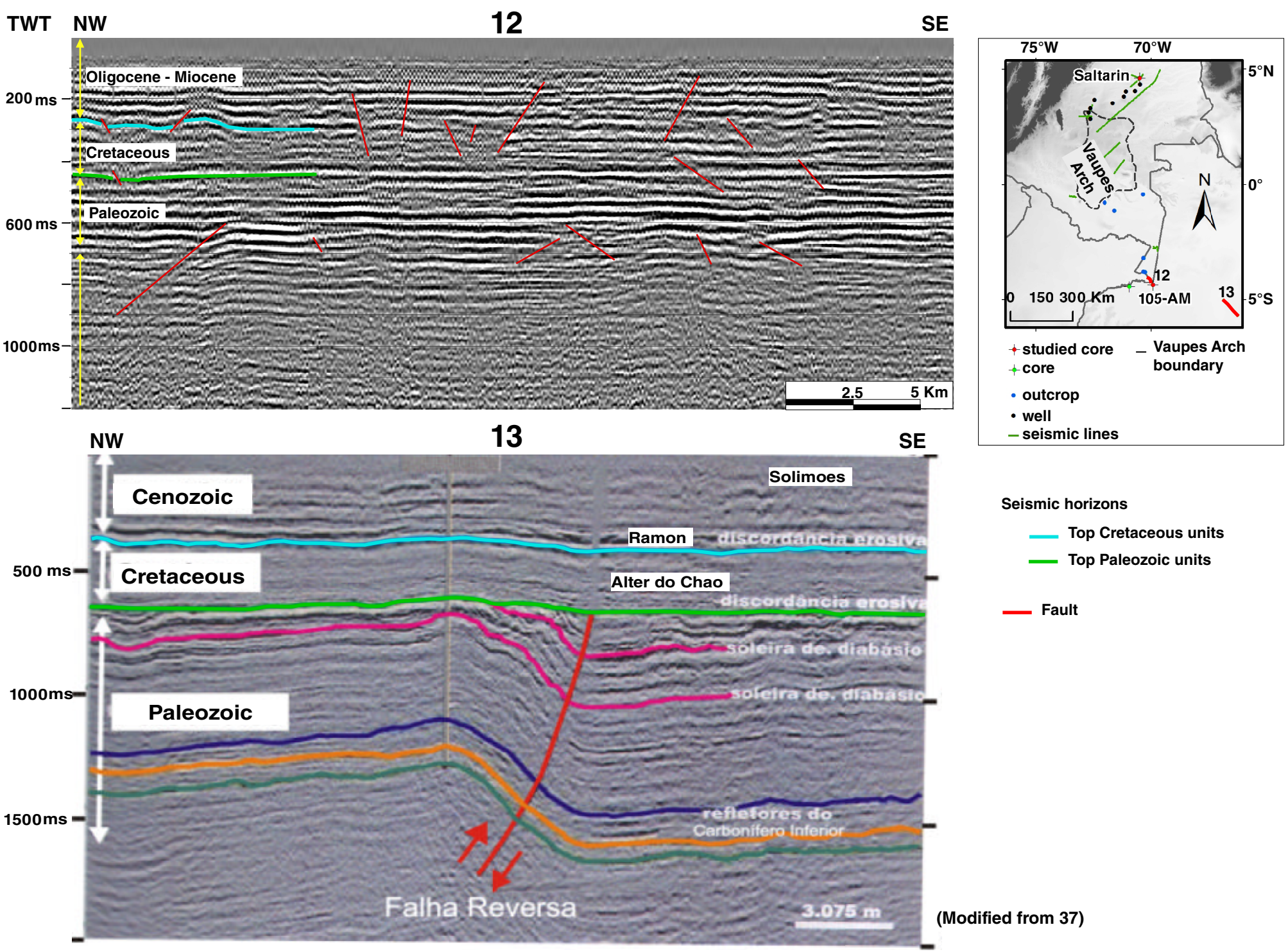

fig. S14. Interpreted 2D seismic profiles showing the contrasting difference of seismic facies between undifferentiated Cenozoic and Cretaceous units in the Amazonas/Solimões Basin (see fig. S2 for location of seismic lines). Cenozoic seismic reflectors are discontinuous and not parallel among them, and the amplitude of the peaks and troughs varies laterally.

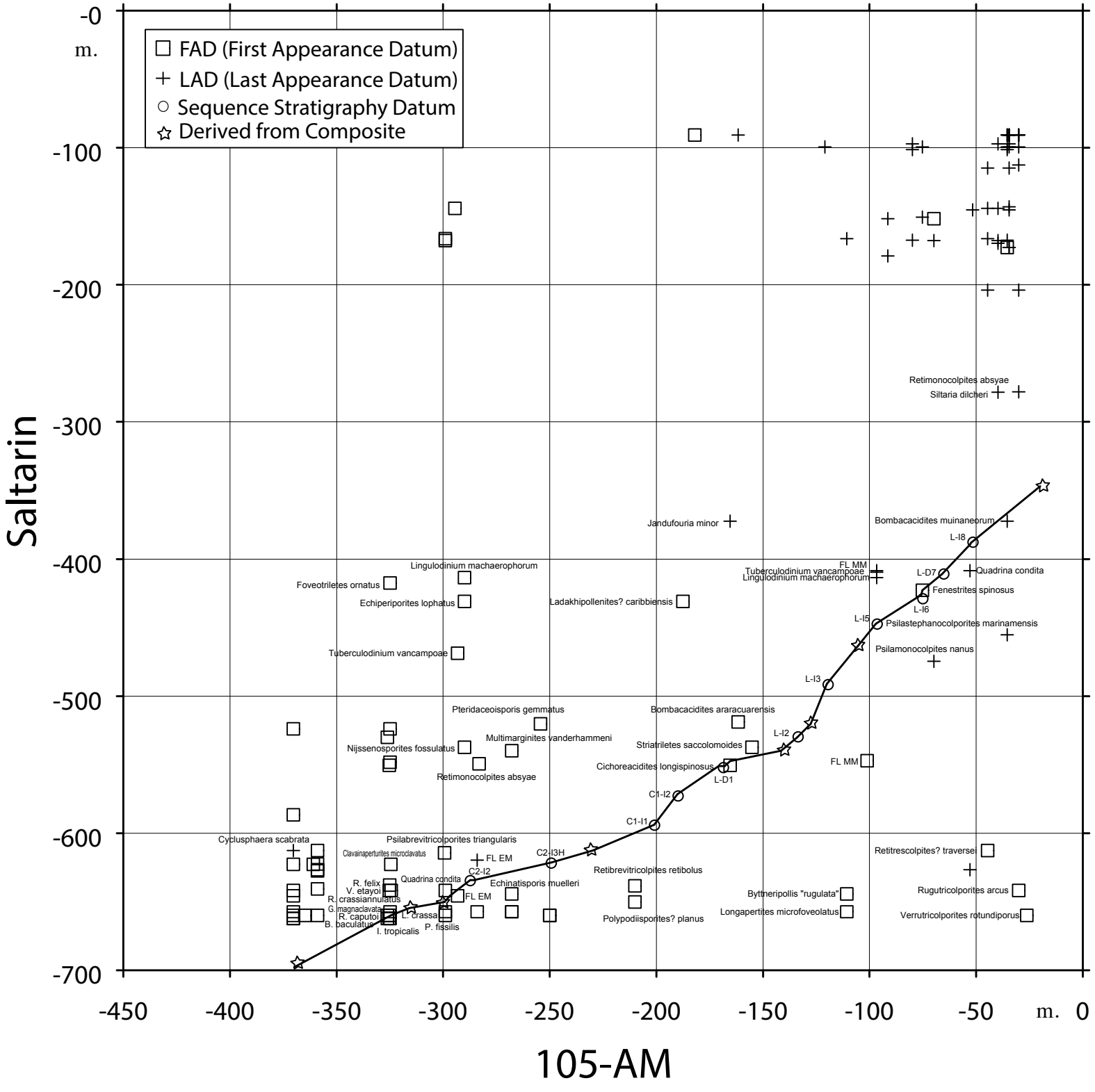

fig. S15. Graphic Correlation between core Saltarin and core 105-AM. Notice the border effect that artificially increases the LAD (Last Appearance Datum) near the top of 105 and increases the FAD (First Appearance Datum) near the base of the section. Line of Correlation is derived from the correlation of both sections among each other, and each individual section versus the Composite (figs. S11 and S12). The segment points of the LOC (Line of Correlation) are in table S9, and all the events of the correlation in this figure are in Supplementary Online File 4.3. (At Dryad Digital Repository, doi:10.5061/dryad.53m76)

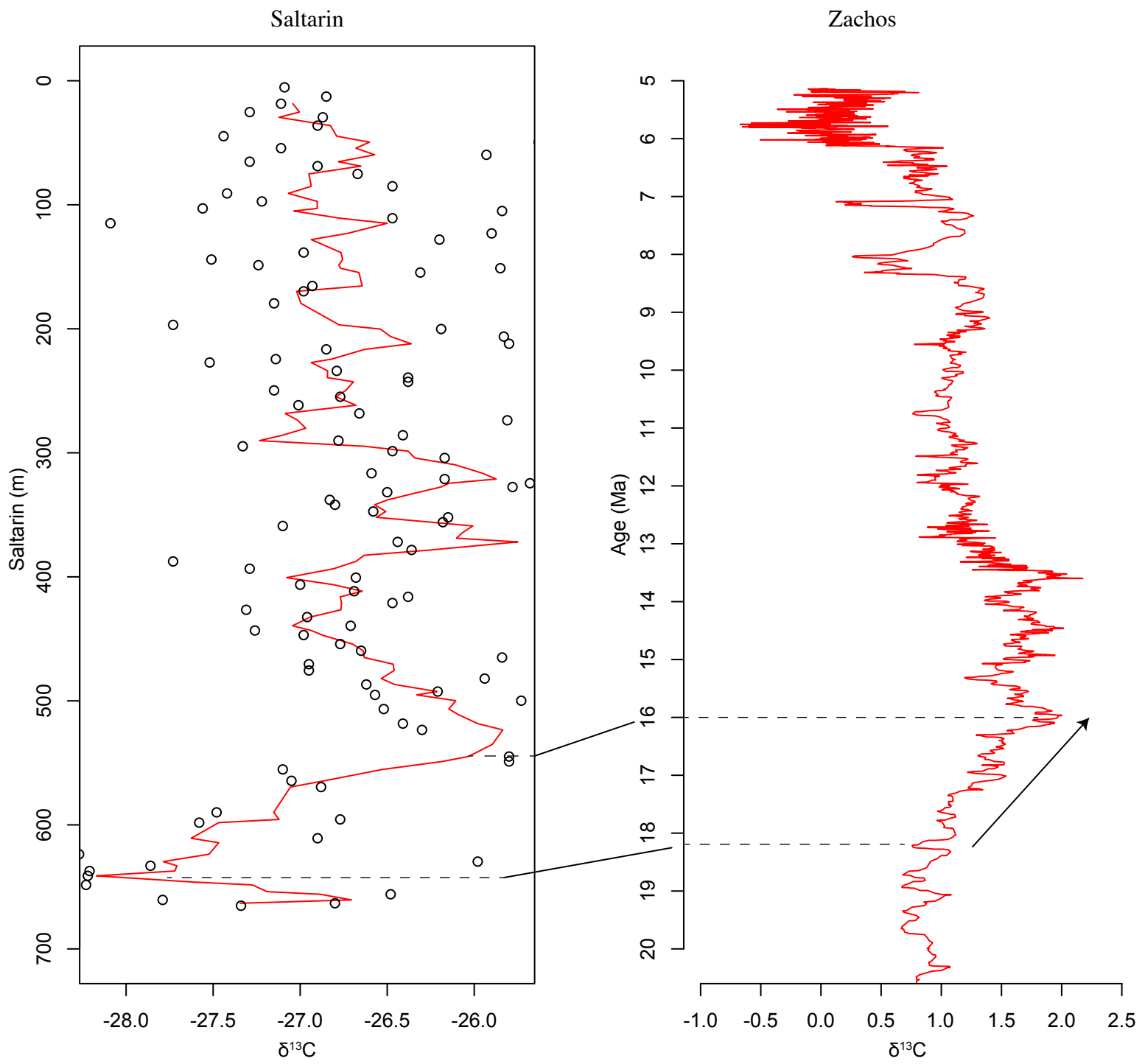

fig. S16. Carbon isotope data (δ13C) versus stratigraphic position in the Saltarin core on the left panel. Raw data and a five-sample running average (red line) shows that there is a positive isotopic shift from meters 637 to 535 (table S6). This shift seems to correspond to the 18 to 16 Ma global positive δ13C shift, right panel *(182)*.

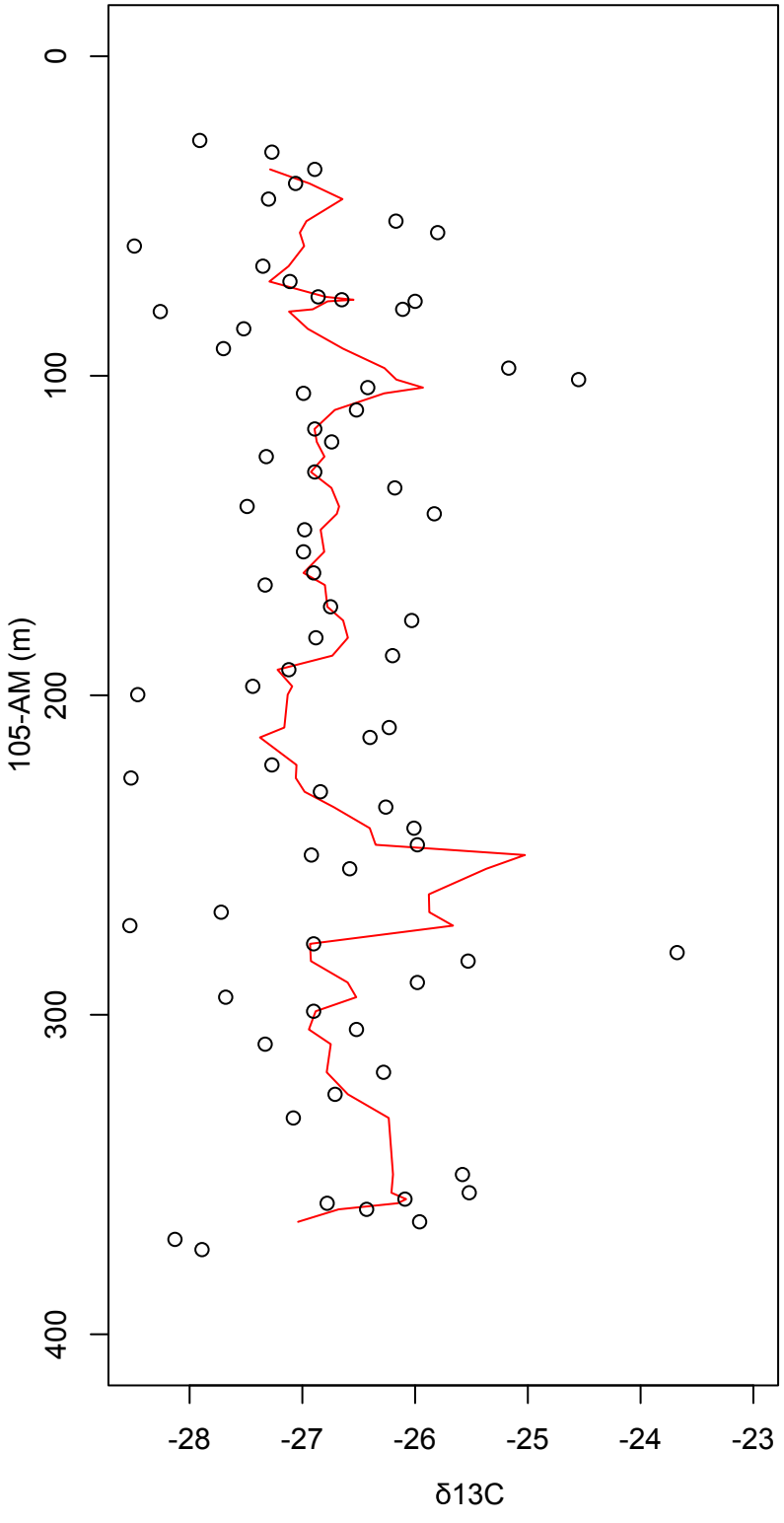

fig. S17. Carbon isotope data (δ13C) versus stratigraphic position in core 105-AM. Raw data and a 5-sample running average (red line) do not show a distinct pattern that could be correlated to the global δ13C record. Sample at meter 262.3 yielded a high value (-19.64 ‰) and therefore it is not plotted in the graphic as it is beyond the X-axis range (-28.5 to -24 ‰).

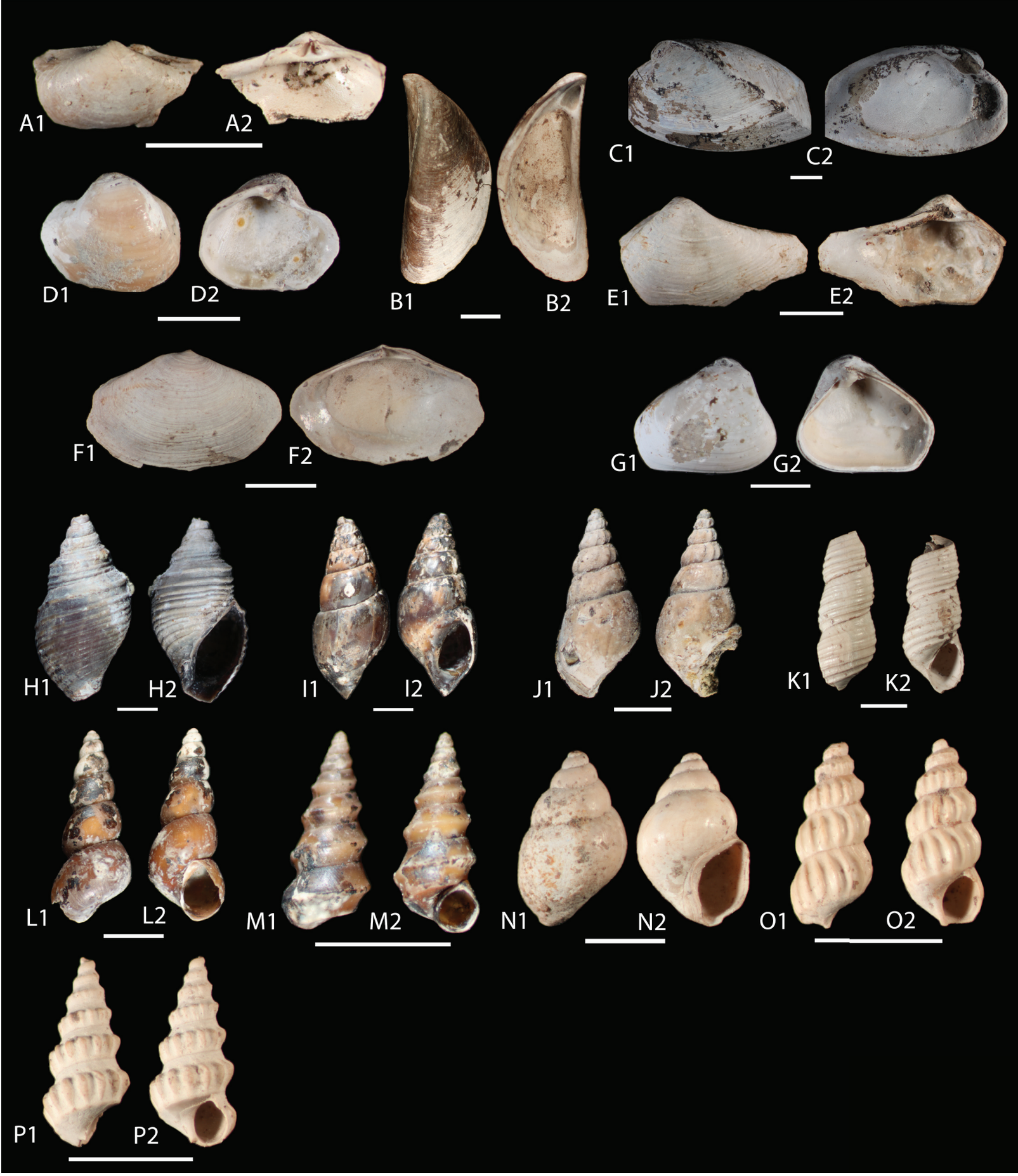

fig. S18. Photographs of shells from core 105-AM. Scale bar is 2.5 mm. (A) to (G) are bivalves for which exterior and interior views are shown (1's and 2's, respectively). (H) to (P) are gastropods for which rear and front views are shown (1's and 2's, respectively). (A) *Corbula cotuhensis* Wesselingh & Anderson, 53 m (B) *Mytilopsis sallei* Récluz, 53 m (C) *Pachydon carinatus* Conrad, 83 m (D) *Pachydon cuneatus* Conrad, 52.9 m (E) *Pachydon ledaeformis* Dall, 53 m (F) *Pachydon telliniformis* Wesselingh, 53 m. (G) *Pachydon trigonalis* Nuttall, 79.9 m (H) *Aylacostoma browni* Etheridge, 53 m (I) *Charadreon glabrum* Wesselingh, 79.9 m (J) *Charadreon intermedius* Wesselingh, 79.9 m (K) *Dyris bicarinatus bicarinatus* Wesselingh, 53 m (L) *Dyris ortoni* Gabb, 79.9 m (M) *Feliconcha feliconha* Wesselingh, 79.9 m (N) *Toxosoma grande* Wesselingh, 53 m (O) *Tryonia nuttalli* Wesselingh, 53 m (P) *Tryonia scalarioides scalarioides* Etheridge, 53 m

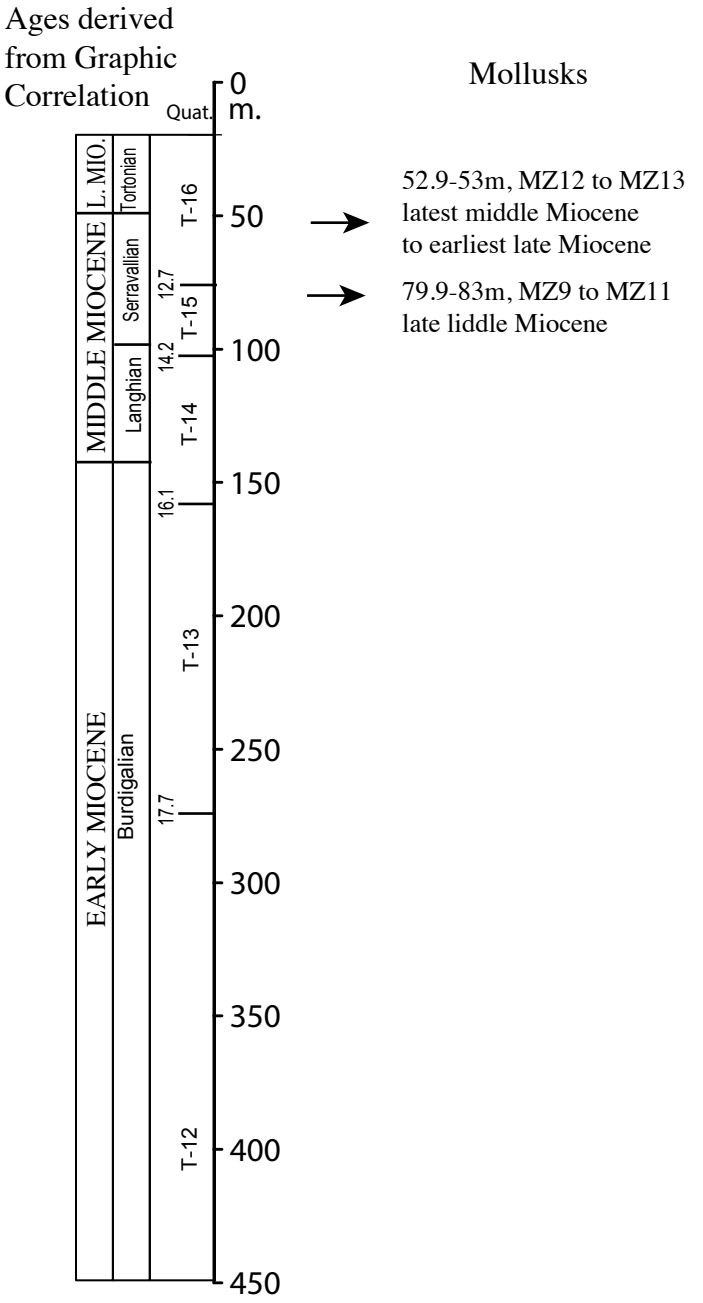

fig. S19. Molluskan biostratigraphy of core 105-AM. Mollusks at meter 52.9-53 indicate zone MZ12 to MZ13 (latest middle Miocene to earliest late Miocene). Assemblage at meter 79.9-83 m indicates zone MZ9 to MZ11 (molluskan Zones after (*71*)). Molluskan biostratigraphy supports the age derived from Graphic Correlation.

table S1. Palynomorph counts for samples analyzed in core Saltarin.
Note= this is a very large table, 140 columns by 640 rows. It is too large to be seen in a Word or PDF file. This table in Excel format is deposited in Dryad Digital Repository, doi:10.5061/dryad.53m76 (Supplementary Online File #6).

table S2. Palynomorph counts for samples analyzed in core 105-AM.
Note= this is a very large table, 97 columns by 512 rows. It is too large to be seen in a Word or PDF file. This table in Excel format is deposited in Dryad Digital Repository, doi:10.5061/dryad.53m76 (Supplementary Online File #6).

table S3. Summary of palynological count data. MP= percentage marine palynomorphs, SD= standard deviation, N= number of samples, N100=number of samples with counts >100, L=percentage lacustrine palynomorphs.

table S4. BIT index for Saltarin samples.

table S5. Geographic coordinates and information of outcrops and wells (coordinate system WGS 1984) used in this study.

table S6. Geographic coordinates and information of 2D seismic lines (coordinate system WGS 1984) used in this study.

table S7. Summary of lithological and palynological indicators for depositional environment interpretation of the Saltarin well. Red color: dominantly Continental environments; black color: dominantly Marginal environments; blue color: dominantly Marginal and Marine environments.

table S8. Summary of lithological and palynological indicators for the depositional environment interpretation of the 105-AM well. Red color: dominantly Continental environments; black color: dominantly Marginal environments; blue color: dominantly Marginal and Marine environments.

table S9. LOC data points for Saltarin versus composite, 105-AM versus composite, and 105-AM versus Saltarin. ID= code of event; Event.Type=type of event; Saltarin.m= stratigraphic position in Saltarin core; 1-AS-105-AM= stratigraphic position in 105-AM core; Composite= composite units of composite section.

table S10. Age of individual samples derived from the graphic correlation analysis. Depth= stratigraphic position, Zones names and number after biostratigraphic zonation of Jaramillo et al. (*56*).

table S11. Total carbon, total inorganic carbon, total organic carbon, total nitrogen, and carbon isotope data for all studied samples.

table S12. Mollusks identified in core 105-AM.

Supplementary Online Files (At Dryad Digital Repository, doi:10.5061/dryad.53m76)

file S1. GPlates project.

file S2. R code.
R code to transfer stratigraphic position into geological time.

file S3. Graphic correlation.
Graphic Correlation Project, includes the software GraphCor needed to run the analysis.

file S4. Events location.
Events of the Line of Correlation for both Saltarin and 105-AM of figs. S12 and S13.

file S5. Lithological description of the cores 105-AM and Saltarin.
It contains the tables needed to reproduce the stratigraphic column of both Saltarin and 105AM of Fig. 1.

file S6. Excel tables.
All supplementary tables in excel format.